International
Progress Report

IPR-01-72

Äspö Hard Rock Laboratory

Evaluation of the interaction of the buffer/rock interaction in the Stripa BMT projekt

Roland Pusch
Geodevelopment AB

Gunnar Ramqvist
Eltekno AB

December 2001

Svensk Kärnbränslehantering AB
Swedish Nuclear Fuel
and Waste Management Co
Box 5864
SE-102 40 Stockholm Sweden
Tel +46 8 459 84 00
Fax +46 8 661 57 19

Äspö Hard Rock
Laboratory

Report no.
IPR-01-72
No.
F107K
Author
Pusch, Ramqvist
Date
01-12-18
Checked by
Date
Approved
Christer Svemar
Date
01-12-19

Äspö Hard Rock Laboratory

Evaluation of the interaction of the buffer/rock interaction in the Stripa BMT projekt

Roland Pusch
Geodevelopment AB

Gunnar Ramqvist
Eltekno AB

December 2001

Keywords: Buffer Mass Test, buffer, bentonite

ABSTRACT

New information is provided on the Buffer Mass Test (BMT), which was focused on the rate of water saturation and associated build-up of swelling pressures in buffer clay. The wetting rate was found to be quickest in three ”wet” holes intersected by water-bearing fractures that are parallel to the major principal rock stress. Holes with perpendicularly oriented fractures gave very slow buffer wetting. The wetting of the buffer in tangential direction was very uniform both in the ”dry” and ”wet” holes, probably due to redistribution of water by a higher average hydraulic conductivity of the rock close to the holes than of the undisturbed rock.

In one hole quicker wetting of the buffer below the heater occurred at a stage when the external water pressure rose and this is assumed to have occurred by leakage through the joints between the blocks. Conceptual models for the wetting of the buffer were proposed for water-bearing fractures intersecting the holes and for fracture-free holes. For the firstmentioned the fracture aperture is believed to be blocked by expansion of contacting forcing water to flow in the excavation-damaged zone thereby causing quick and uniform wetting of the buffer. For holes with no intersecting water-bearing fractures the wetting is caused by water being forced through the tight rock matrix which causes slow wetting.

LIST OF CONTENTS

SAMMANFATTNING

Denna rapport innehåller delvis ny information om fältundersökningen Buffer Mass Test (BMT), som utgjorde en fas i Stripaprojektet. BMT var fokuserat på bestämning av hastigheten hos vattenmättnaden och uppbyggnaden av svälltryck i högkompakterad buffertlera av MX-80 bentonit. I nu föreliggande studie var intresset koncentrerat på att finna om och hur buffertbevätningen kan relateras till bergets struktur och konduktivitet. BMT-försöket hade stora likheter med Prototype Project med 6 värmare men var i skala 1:2. Bevätningen av bufferten befanns vara betydligt snabbare i hålen med sprickor orienterade NW/E till NW/SE, dvs i största huvudspänningens riktning, än i hål som innehöll sprickor orienterade NE/SW. Det visar att de förstnämnda förde mer vatten vilket kan förklaras av bergspänningssituationen. Bufferten i de ”våta” hålen blev nästan helt vattenmättad på 3 år och ett svällningstryck av 10 MPa byggdes upp på halva värmarhöjden efter ungefär 30 månader. En viktig slutsats var att bufferten i ett framtida KBS-3-förvar bör bli vattenmättad på några få år om deponeringshålen genomskärs av vattenförande sprickor medan det kan ta flera decennier för att nå buffertmättnad utan sådana sprickor. Detta gäller med reservationen att vattentryckets storlek kan komma att påverka bevätningstakten.

Bevätningen av bufferten i tangentiell riktning var mycket jämn både i de ”torra” och ”våta” hålen vilket antyder omfördelning av vatten på grund av högre hydraulisk konduktivitet hos omgivande närfältberg än hos det ostörda berget. Det är möjligt att det inte bara är fråga om en ytlig, mekanisk störd zon utan också en förhöjning av konduktiviteten till några decimeters avstånd som tillsammans bidrar till fördelning och transport av vatten från enskilda vattenförande sprickor

Vattenkvotkurvorna för bufferten på halva värmarhöjden och svälltrycksuppbyggnaden visar en långsam kontinuerlig vattenupptagning från berget i de ”torra” hålen. De flesta kurvorna har en för diffusion karakteristisk form medan de som illustrerar bevätningen av bufferten under värmarna, där temperaturgradienten var mindre, antyder att vattenupptagning delvis skett genom att vatten i ett tidigt skede vandrat eller tryckts in i fogarna mellan blocken.

I ett av hålen var bevätningen olika snabb i två påföljande försöksserier. Det första gjordes med 600 W effekt som gav långsammare bevätning än det efterföljande försöket med 1200/1800 W effekt trots att viss avdunstning då bedöms ha ägt rum. Det ökade inflödet till detta hål kan förklaras av att omstyrning av grundvattnet i omgivande berg gett ett dokumenterat förhöjt vattentryck med åtföljande inpressning av vatten i fogarna mellan blocken.

På basis av observationerna föreslås konceptuella modeller för buffertbevätning. I fallet med vattenförande sprickor som skär deponeringshålen är det möjligt att spricköppningarna blockeras av expanderande lera som är i kontakt med öppningarna och tvingar tillströmmande vatten att transporteras i den störda zonen med jämn och snabb bevätning av bufferten som följd. I fallet utan sådana sprickskärningar orsakas buffertens bevätning av vatten som tvingas genom den täta bergmatrisen, vilket ger långsam bevätning.

SUMMARY

The present document contains partly new information on the Buffer Mass Test (BMT), performed as one phase of the Stripa Project. The BMT focused on the rate of water saturation and associated build-up of swelling pressures in highly compacted MX-80 bentonite buffer. The main interest in the present context was to see if and how the wetting of the buffer clay could be related to the rock structure and conductivity. The experiment was very similar to the present Prototype Project with 6 heater holes, but was on a 1:2 % scale. The wetting rate of the buffer clay was found to be much quicker in three holes with NW/E to NW/SE oriented major fractures, i.e. those parallel to the major principal stress, than in holes that were only intersected by fractures oriented NE/SW. This indicates that the firstmentioned fractures carried more water than the others, which is explained by the rock stress situation. The buffer in the ”wet” holes was almost completely saturated in 3 years and a stable swelling pressure of around 10 MPa was built up after about 30 months at mid-height of the heaters. A major conclusion was that the buffer in a future repository of KBS-3 type will be hydrated in a few years if the deposition holes are intersected by water-bearing fractures, while it may take decades to get the buffer saturated in holes with no such features. This is, however, with the reservation that high water pressures may affect the buffer saturation rate.

The wetting of the buffer in tangential direction was very uniform both in ”dry” and ”wet” holes and this seems to be due to redistribution of water by a higher average hydraulic conductivity of the rock close to the holes than in the undisturbed rock. It is possible that there is not only a shallow mechanically damaged EDZ but also a stress-generated zone of disturbance with somewhat higher conductivity than of undisturbed rock, extending to a few decimeters from the periphery and assisting in distribution and transport of water from discrete water-bearing fractures.

The plotted water content at mid-height of the heaters in the ”dry” holes and the swelling pressure measurements show a slow but continuous uptake of water from the rock. Most of the wetting curves are diffusion-like, while those representing the buffer below the heaters, where the temperature gradient was lower, have a different shape suggesting that water leaked or was pressed into the joints between the buffer blocks at an early stage.

In one hole the rate of wetting was different in two consecutive test series. The first test with 600 W power gave slower wetting than the subsequent test with 1200/1800 W power despite the desiccation that is believed to have occurred in the hot test. The documented increased flow to the hole in the second test can be explained by redirection of water yielding an increased water pressure that caused penetration of water into joints between the buffer blocks.

On the basis of the observations conceptual models for the wetting of the buffer were proposed. For the case of water-bearing fractures intersecting the holes it is believed that the aperture was blocked by expansion of contacting forcing water to flow in the excavation-damaged zone thereby causing quick and uniform wetting of the buffer. For holes with no intersecting water-bearing fractures the wetting is caused by water being forced through the tight rock matrix which causes slow wetting.

1 INTRODUCTION

Prediction of the rate of water uptake of the clay buffer surrounding the canisters in KBS-3 holes requires that the hydraulic interaction of the buffer and the surrounding rock is understood and can be quantified. The Stripa BMT test provides numerous data that can be used for calibration of existing theoretical models and development of new ones. It is therefore believed to be useful for the modelling groups in the Prototype Repository Project.

The present report describes the BMT project with particular emphasis on the hydraulic interaction between the rock and the buffer. A number of the data used here are found in the final reports of the Stripa Project [1,2,3] but various raw data, listed in preliminary and internal reports were also used.

The BMT field experiment was an approximately half-scale version of a KBS-3 repository except for the size of the horseshoe-shaped tunnel, which had 5 m height and width.

Since the present study is focused on the interaction of buffer and rock with respect to water transport and mechanical performance, characterization of the rock and interpretation of the buffer/rock interaction mainly concerns the heater holes and – in particular – those parts of the holes that are located below the blast-induced EDZ.

2 ROCK CHARACTERIZATION

2.1 General

For description of the structural build-up of rock one can use the general categorization scheme in Table 2-1 and this scheme has been applied in this report. Low-order discontinuities, which are faults (1st order), major fracture zones (2nd order), and minor fracture zones (3rd order), are characterized by typical hydraulic conductivity and strength properties. High-order discontinuities - fractures, fissures and pores - are discrete discontinuities that control the bulk properties of rock located between those of low order.

According to SKB's strategy discontinuities of 1st and 2nd orders should not intersect deposition tunnels and holes while those of 3rd order may intersect deposition tunnels. 4th and higher order discontinuities have to be accepted in deposition holes. Discontinuities of higher orders than 4 are only slightly hydraulically active but may still play a role in supplying the buffer clay with water by undergoing stress-induced propagation and aperture changes.

Table 2-1. Categorization scheme of discontinuities [4]. 1st to 3rd are zones,4th to 7th are discrete fractures. VH=very high, H=high, VL=very low, L=low, M=medium.

Order	Persistence	Average hydraulic transmissivity	Gouge content	Strength
1st	>Kilometers	Very high	Very high	Very low
2nd	Kilometers	High	High	Low
3rd	Hundreds of meters	High to medium	High to medium	Low to medium
4th*	Tens of meters	Medium	Medium to low	Medium to high
5th*	Meters	Low	Very low	Medium to high
6th*	Decimeters	Very low	Insignificant	High
7th*	<Decimeters	Insignificant	None	Very high

* Physical properties refer to rock without discontinuities of lower order

2.2 The BMT drift

2.2.1 General

The BMT drift was located at 360 m depth several hundred meters from the mined-out ore body. It had been used for field experiments ("Ventilation Test") by the Lawrence Berkeley Laboratory (LBL) and long boreholes that had been drilled for piezometric measurements in these tests. The 6 heater holes (0.76 m diameter and 3 m depth) in the BMT experiment are shown on LBL's drawing in Figure 2-1.

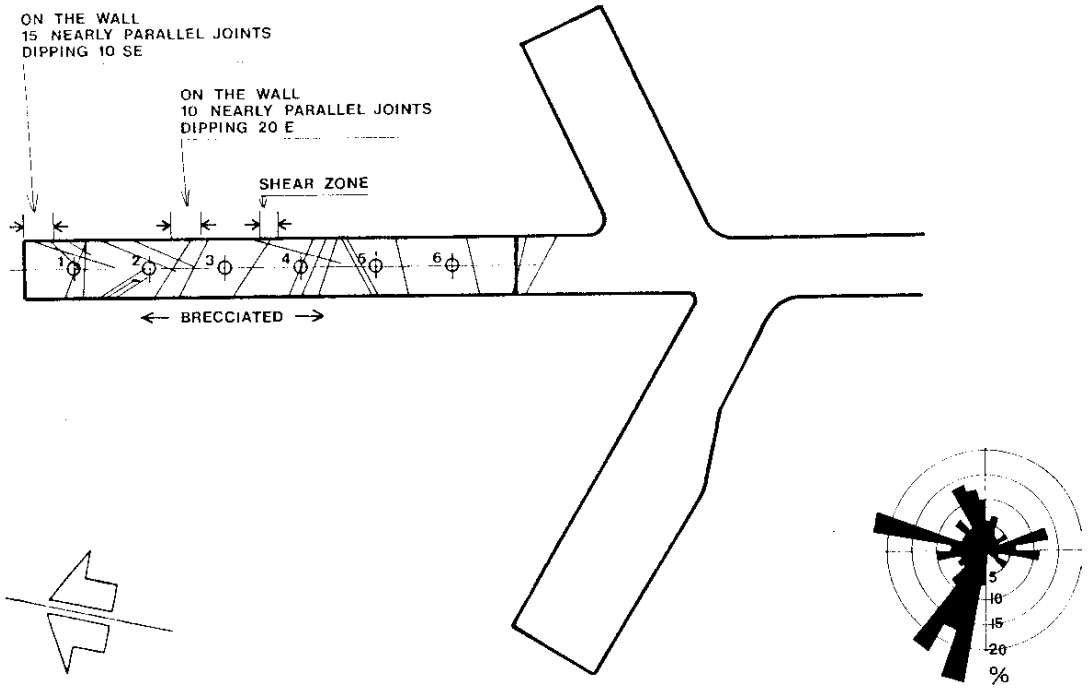

Figure 2-1*. Plan view of the nearly horizontal BMT drift. The rose shows that the majority of the fractures are oriented W/E to NW/SE [5].*

2.2.2 Rock material

The rock evolved as a granite dome with the major petrographic constituent being medium-grained monazite with a grain size of about 3 mm. Major minerals are quartz (35-44 %), feldspars (59-61 %), chlorite and muscovite (5 %).

Laboratory tests have given the following data [5].

Youngs' modulus: E=51.3 GPa
Poisson's ratio: ν=0.23
Density: ρ=2622 kg/m^3
Unconfined compression strength: C_o=210 MPa,

2.2.3 Rock stress conditions

Measurements

The primary rock stress conditions in the Stripa granite have been determined by stress measurements in a horizontal boreholes extending from a drift at 360 m depth located about 40 meters from the BMT drift, and in a vertical boreholes immediately north of the 3D drift, about 400 m from BMT. The latter measurements were made by applying hydraulic fracturing and are believed to be most representative of the general stress field, which has the following components (horizontal and vertical directions), [5]:

σ_{Hmax}=10 + 0.0939x360. Average 22 MPa, oriented N65^{o}W (nearly WNW)
σ_{Hmin}=1.69 + 0.0299x360. Average 12 MPa, oriented N35^{o}E (nearly NNE)
σ_{Vert}=3.6x2.5721. Average 5 MPa

The rock stresses have been reported to vary both with respect to magnitude and orientation [5], an example being the results from measurements in a 20 m long horizontal borehole [6]. They showed that the major principal stress had an average value of about 19 MPa but varied between 25 and 15 MPa excepting a few extreme values. The intermediate principal stress had an average value of about 9 MPa with a variation from 5 to 15 MPa, while the minor principal stress was in the range of 2 to 8 MPa. The measurements in this borehole indicate very significant stress variations possibly due to the presence of a diabase dike and the influence of mining operations.

The obvious winding of major fracture sets is believed to indicate variations in the orientation of the stress field, partly or largely reflecting the conditions at the formation of the rock mass [7].

2.2.4 Piezometric conditions

The water pressure has been measured in deep and shallow boreholes and in a large number of boreholes in the test areas at 300 to 400 m depth. At several hundred meters distance from mined rooms and many tens of meters from test drifts water pressures up to 3 MPa have been recorded. The pressure was typically in the interval 0.7 to 1.3 MPa at a distance of 1-2 meters from the TBM drift [8].

The piezometric conditions in the near-field of the six heater holes were estimated as summarized in Table 2-1.

Table 2-2. Estimated water pressure in kPa at the base of the heater holes as a function of time [3].

Hole	Initial	3 months after start of the respective test	6 months after test start	12 months after test start	24 months after test start
1	0	710	750	700	780
2	0	490	495	430	540
3	0	30	20	15	-
4	0	220	645	630	-
5	0	300	500	620	485
6	0	30	20	15	15

The data indicate that the water pressure at the base of the holes approached its final value very early in Holes 1 and 2, while it took half a year to be built up in Holes 4 and 5. The pressure in Holes 3 and 6 never reached higher than about 30 kPa.

3 HYDRAULICALLY ACTIVE STRUCTURAL COMPONENTS IN THE ROCK

3.1 Regional discontinuities

The tectonic history involved deformation along Precambrian faults zones and movements in conjunction with the upraisal of the Swedish/Norwegian border mountains in Tertiary time and in conjunction with glaciation and deglaciation in Quaternary time.

There are major lineaments in the area, a dominant one being the N- to NNE-oriented lake Råsvalen. This discontinuity has an extension of tens of kilometers and represents a 1st order discontinuity. West of the northern end of Råsvalen the pattern of large-scale discontinuities is illustrated in Figure 3-1. They represent 2nd order discontinuities and are oriented NW/SE and NE/SW and have a spacing of about 1 km. Minor fracture zones representing 3rd order discontinuities have approximately the same orientation as the larger ones and have an average spacing of 75 m in the Stripa area. The implications of the large-scale structural network is that the groundwater level in the area is high and that there is rich access to water in the Stripa area as manifested by the fact that it became largely filled with water within less than 10 years after abandoning it.

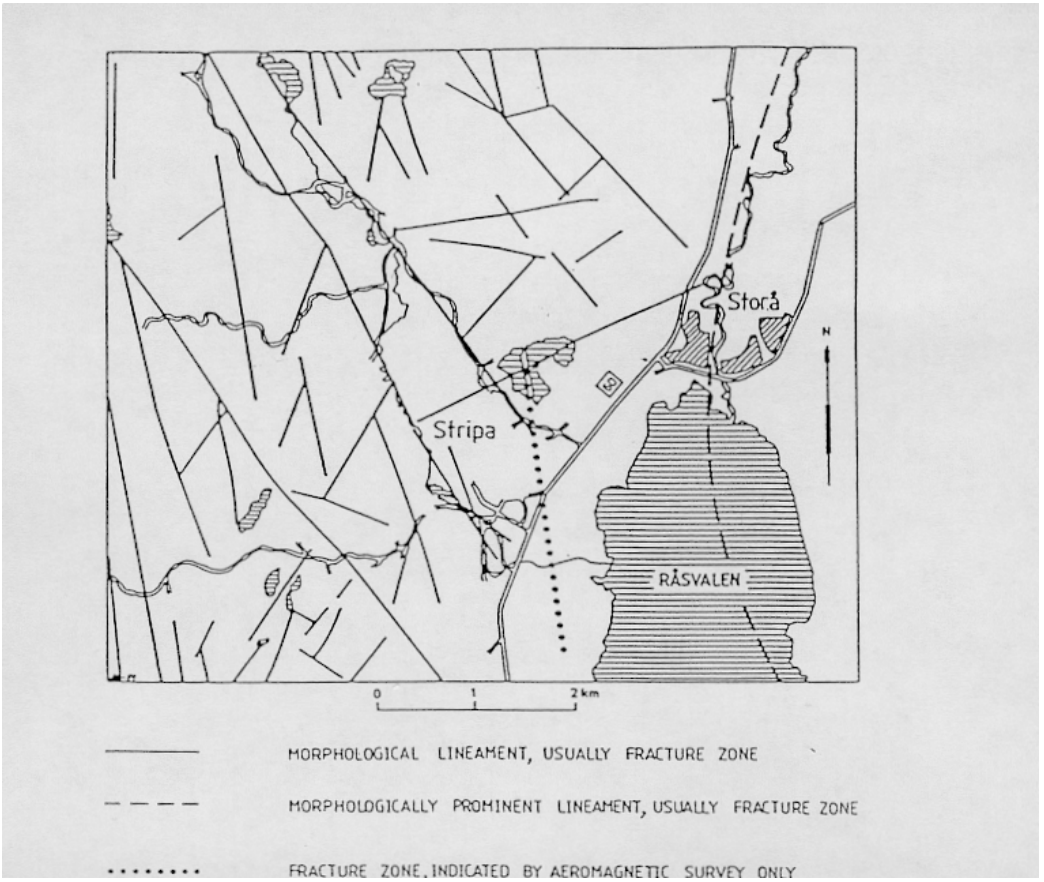

Figure 3-1. *Major discontinuities in the Stripa region. The full lines represent 2nd order discontinuities with a length of 1 to 10 km, while the broken curved line through Råsvalen is a fault of 1st order [9].*

3.2 Buffer Mass Test area

3.2.1 Low-order discontinuities

The test drift is intersected by one 3rd order fracture zone with a width of about 0.5 m. It is represented by the two parallel and closely located NW/SE fractures that intersect Hole 2 in Figure 3-1.

3.2.2 High-order dicontinuities

A fairly complete picture of the system of 4th and higher order discontinuities is obtained by combining core data and mapping of rock exposed in tunnels and drifts and work of this type was performed in the joint Swedish-American Cooperative Program on Radioactive Waste Storage in Mined Caverns at Stripa. It concerned discontinuities with a trace length of at least 0.5 m, representing 4th and 5th order discontinuities. They were found to make up 4 major sets as specified in Table 3-1.

Table 3-1. Geometrical data of fractures with a trace length of at least 0.5 m in Stripa granite [9].

Set no	Mean vertical spacing, m	Mean dip angle (°)	Normal spacing, m	Trace length, m, Median	Trace length, m, Lower quart.	Trace length, m, Upper quart.
1	0.73	41	0.55	1.1	0.5	3
2	0.50	59	0.25	0.8	0.5	2
3	0.32	39	0.25	0.8	0.4	1.2
4	0.42	0	0.42	-	-	-

Table 3-1 suggests that about 25 % of all fractures belonging to Sets 1-3 have a trace length of less than 0.5 m and that 25 % persist for more than about 1-3 m. The total number of fractures exposed on a 100 m^2 randomly oriented wall is expected to be 100-200. Only 10 % of them, i.e. 10 to 20, persist for more than 5 m and have a spacing of at least 2 m, representing hydraulically important fractures, i.e. 4th order discontinuities. Similarly, a cross section area of 7.5 m^2, representing the wall area of a BMT heater hole, would be expected to show 0.7 to 3 fractures of 4th order. It means that the average number of such fractures intersecting the heater holes would be 1 to 2, and that one or two out of the six actually bored holes would have no fracture at all of this type. This is in fair agreement with the actually identified features, which indicates that the rock structure in the BMT area is of the same type as that of the Stripa rock in general.

Applying these data one would expect the floor of the 35 m long and 5 m wide test drift, which has an area of 175 m^2, to be intersected by at least 15 discontinuities of 4th order. Mapping has shown it to be intersected by only 12 fractures of this type (Figure 3-1), which hence demonstrates that the BMT drift has relative few major water-bearing fractures.

3.2.3 Near-field rock structure – 4th order discontinuities

Since the present study concerned the interaction of buffer and rock with respect to water transport and mechanical performance, characterization of the rock and interpretation of the

buffer/rock interaction are confined to the heater holes and – in particular – those parts of the holes that are located below the blast-induced EDZ. The bulk hydraulic conductivity and frequency of fractures in cores drilled from the floor of the drift [8,9] showed that comprehensive disturbance of the rock had taken place by the blast-excavation down to about 1.5 m below the floor. Thus, only the parts of the rock located below 1.5 m depth are considered in the present report.

The presence of hydraulically important discrete fractures, i.e. those of 4th order, is shown for the six heater holes in Figures 3-1 to 3-3.

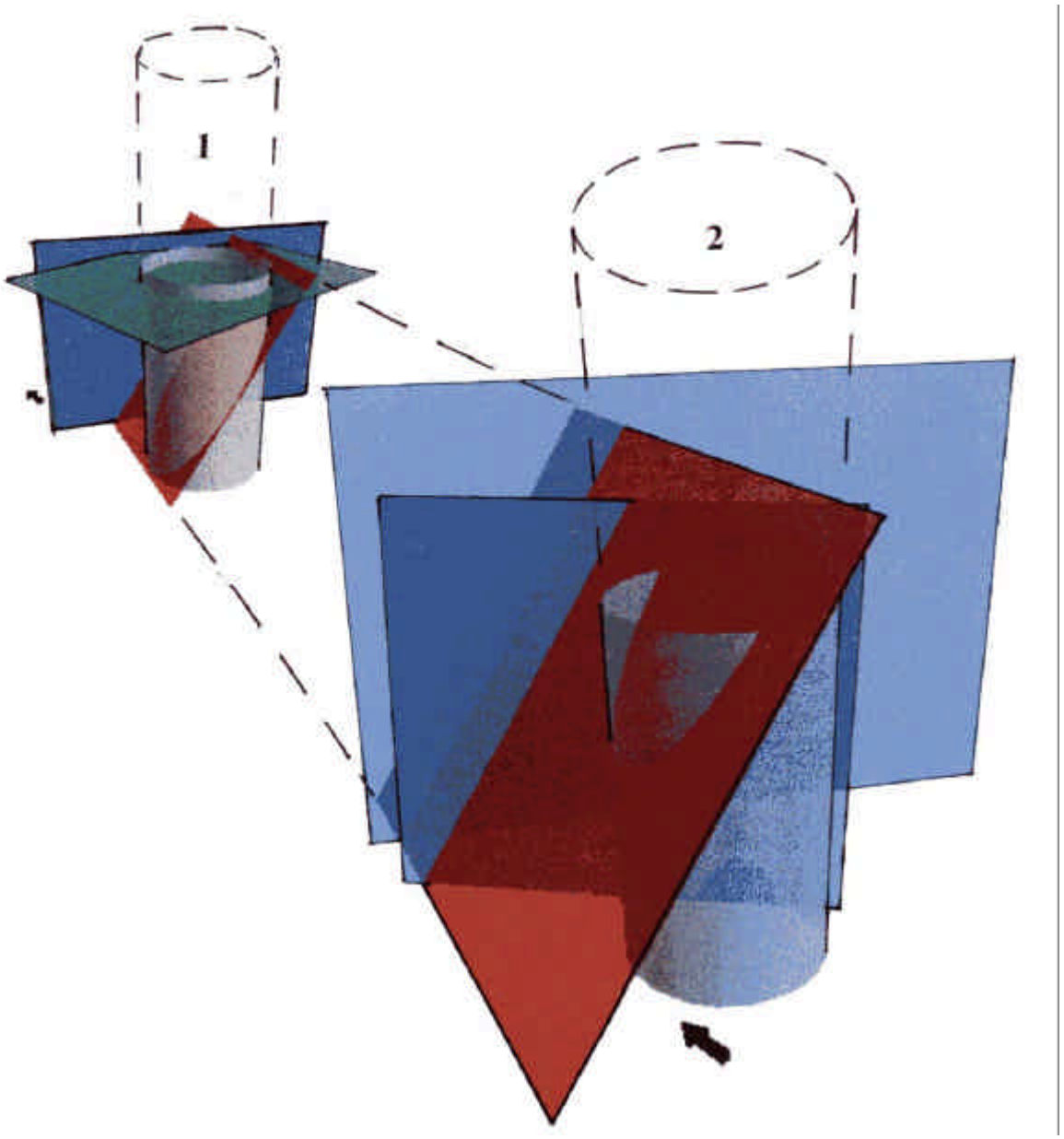

Figure 3-1. *4th order fractures intersecting Holes 1 and 2 below 1.5 m depth. The blue fractures are oriented NW/SE and the red ones NE/SW. The green fractures are subhorizontal. Both holes are intersected by three fractures, Hole 2by two NW/SE-oriented ones. Arrows indicate north direction.*

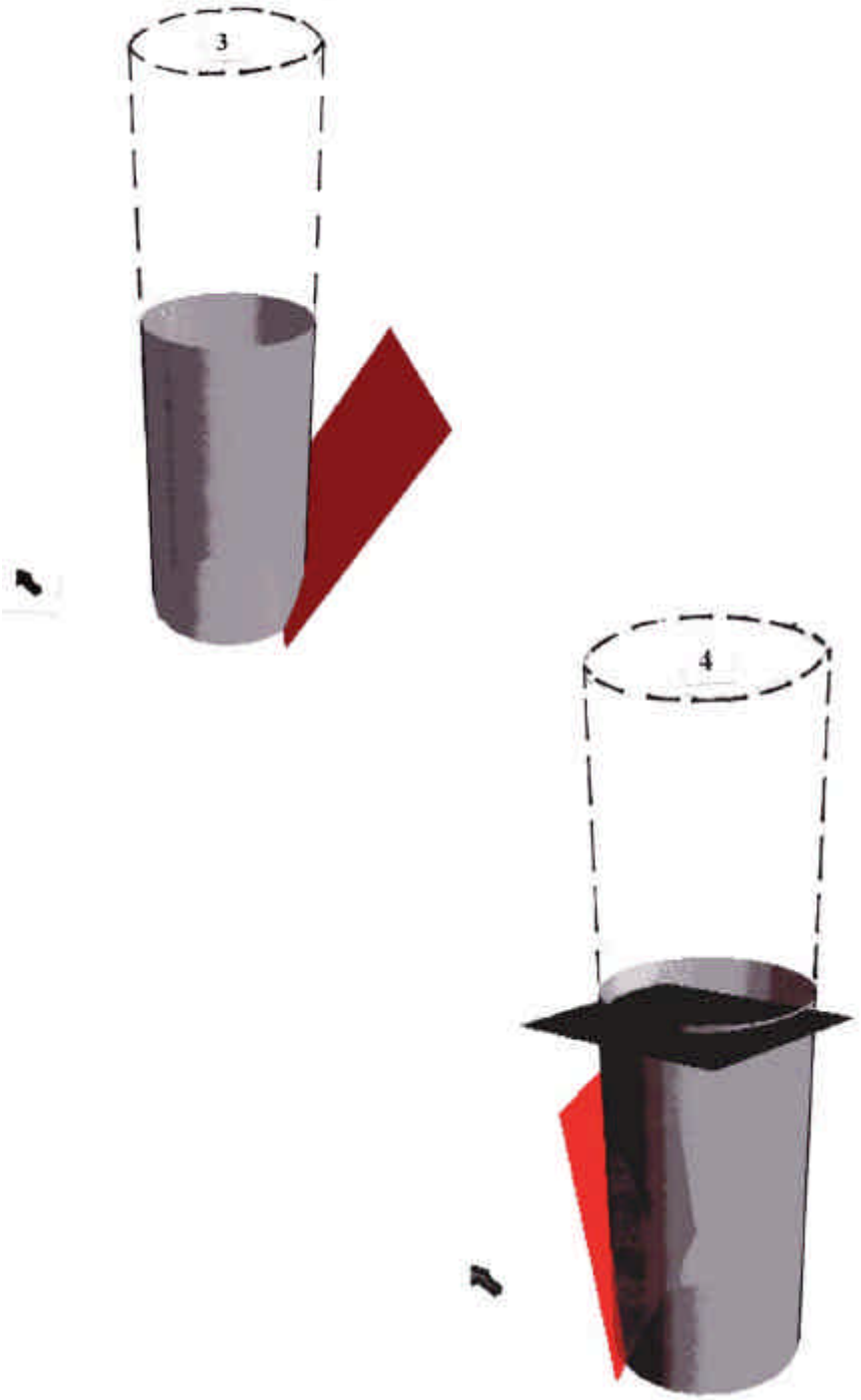

Figure 3-2. *4th order fractures intersecting Holes 3 and 4 below 1.5 m depth. Hole 3 is intersected by only one (red) fracture, which is oriented NE/SW like the one in Hole 4. The latter hole is intersected also by a subhorizontal (green) fracture. Arrows indicate north direction.*

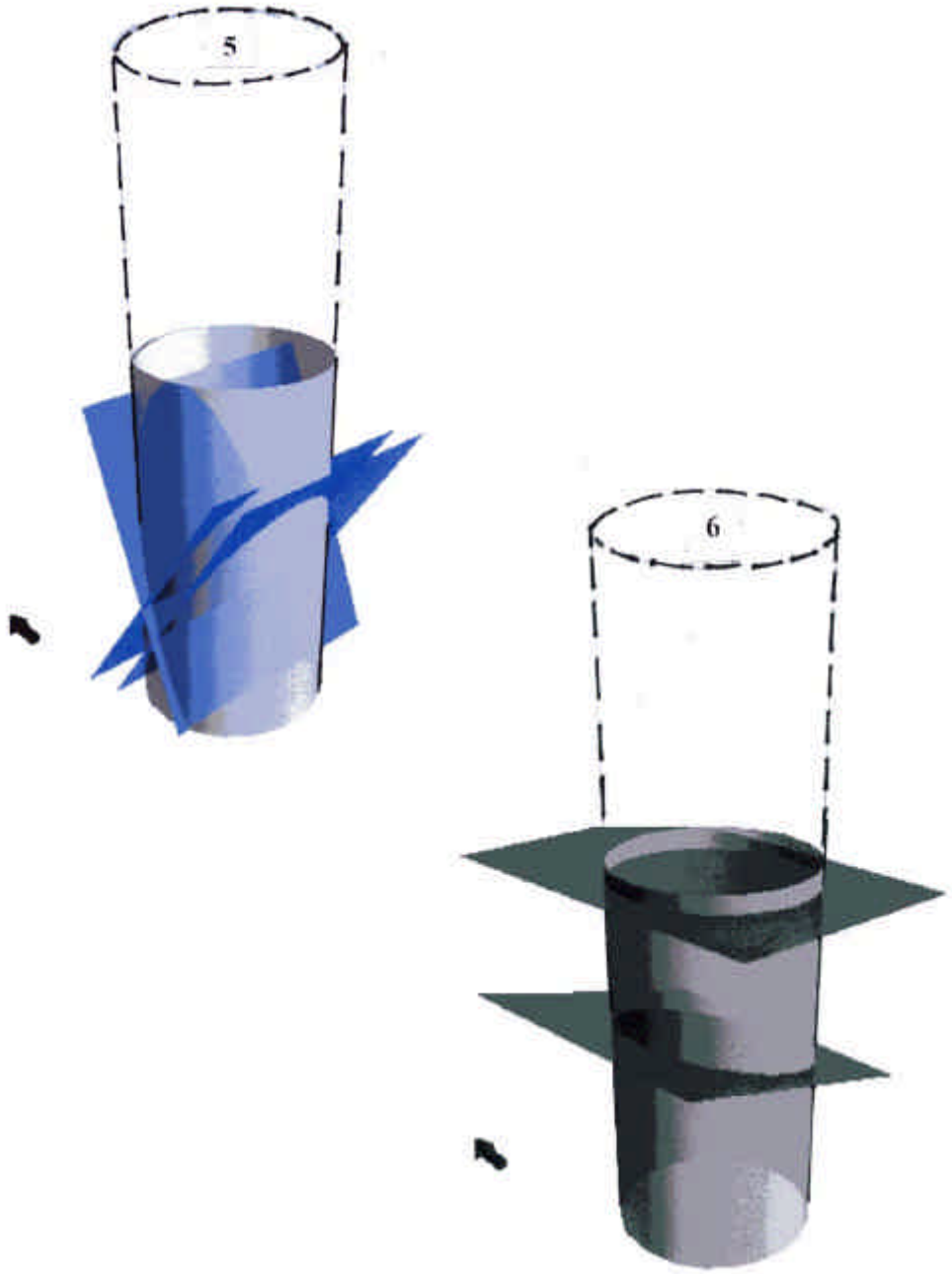

Figure 3-3. *4th order fractures intersecting Holes 5 and 6 below 1.5 m depth. The blue fractures in Hole 4 are oriented WNW/ESE and NW/SE. The holes are not intersected by any NE/SW-oriented (red) fractures. Hole 6 is intersected only by two subhorizontal (green) fractures. Arrows indicate north direction.*

3.2.4 Near-field rock structure – the EDZ

Observation of the flow of water from fractures usually shows dripping from certain spots, particularly from voids formed where fractures intersect, but water can be assumed to be effectively transported along their entire length since the fracture fillings, usually chlorite, epidote and calcite, are richly fissured (Figure 3-4) and because the shallow part of the fractures are eroded by the combined mechanical and hydraulic impacts of the boring process.

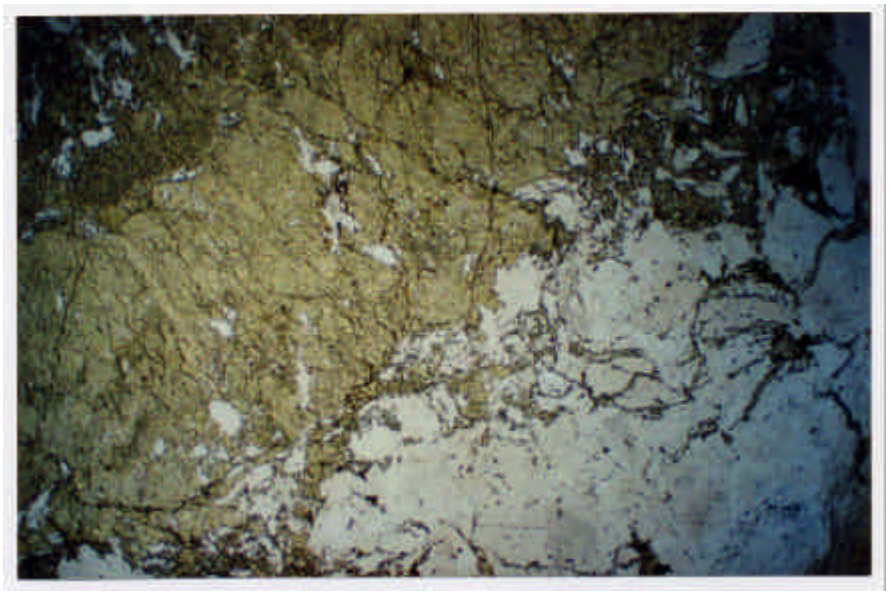

Figure 3-4. *Photographs of fracture fillings. Upper: SEM picture of porous chlorite filling in 4th order fracture (Forsmark). The bar is 10 µm. Lower: Light microscope picture of thin section showing richly fissured epidote fracture filling of Stripa type (green, fissures are black). Magnification about 100 x.*

Examination of the big cores from the drilling of the BMT holes showed that a number of finer fractures with limited water-bearing capacity, i.e. of 5th order, were partly open because their fillings had been eroded by the combined mechanical and hydraulic impacts of the boring to a depth of a millimeter or more (Figure 3-5). They hence have a potential of transporting water along their exposed length in the walls of deposition holes, thereby representing flow paths in the shallow boring-disturbed zone. For the rock in Figure 3-5 the spacing of clearly discernible discontinuities of this type was on the order of 50 mm.

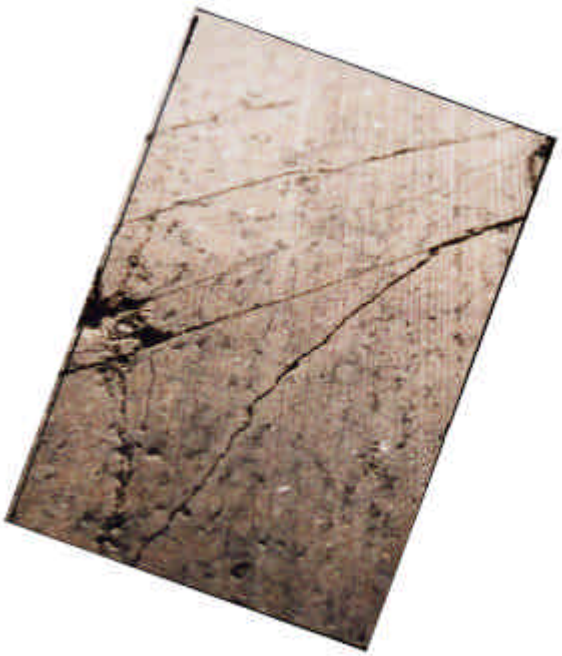

Figure 3-5. *Photograph of curved surface of big core extracted from 0.76 m diameter core-drilled deposition hole in Stripa granite. The short edge of the picture is about 20 cm. It depicts at least 6 chlorite-filled more or less parallel fractures of 5th and 6th orders and some hundred finer breaks. Notice the breakage and loss of rock material where a 4th order fracture intersects two of the finer fractures (lower left).*

3.3 Hydraulic measurements in the heater holes

3.3.1 Procedures

Information on the hydraulic performance of the near-field rock was obtained by recording the inflow into the holes and by performing packer tests in two of them. The inflow measurements were made by use of a movable funnel [1] the results being summarized in Table 3-2 for the lower half of the holes, i.e. from 1.5 to 3 m depth. These tests were not altogether successful because of practical difficulties and more characteristic data are believed to be those performed in pilot boreholes drilled before the full-size holes. They show that the rock where Holes 1, 2 and 5 were subsequently drilled was significantly more water-bearing than where the remaining holes were located.

Table 3-2. Inflow in Holes 1 to 6 [1].

Hole No	Inflow, liters per day from 1.5 to the bottom	Inflow in pilot boreholes, liters per day
1	2.8	6.2
2	2.8	5.6
3	*	3.0****
4	**	0.2
5	***	1.9
6	1.0	0.2

* Not measured because of practical difficulties.
** Water leakage from previously drilled deep pilot hole.
*** Only the inflow from the entire hole length was made.
**** Overrated because of inflow from the richly fractured part down to 0.5 m from the tunnel floor.

The packer tests in Holes 1 and 2 were performed in a Stripa project that was made after the BMT test and was part of an experiment for finding out how effectively the rock around large-diameter holes can be grouted [3]. Figure 3-6 illustrates the equipment and Table 3-3 the evaluated hydraulic conductivity of the rock around the holes.

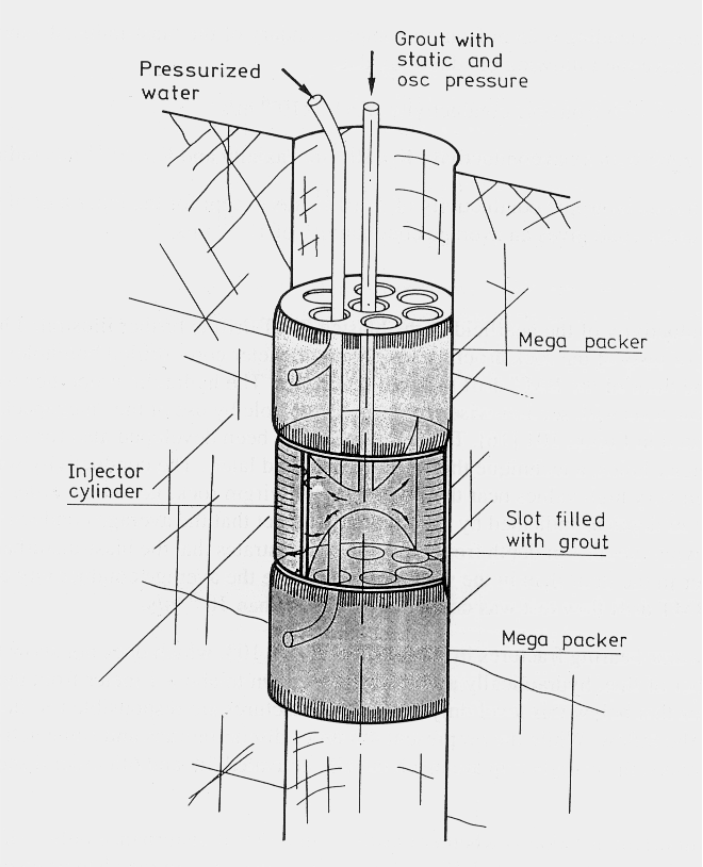

Figure 3-6. *"Megapacker" for determination of the hydraulic conductivity of the rock around two big holes (No 1 and 2) before and after grouting that was also made by use of this equipment.*

Table 3-3. Evaluated hydraulic conductivity in m/s of the ”megapacker” tests before grouting [3].

Hole No	Depth 1.3-1.5 m	Depth 1.7-2.0 m	Depth 2.0-2.3 m
1	7E-8	8E-8	7.5E-8
2	6E-7	7E-9	7.5E-9

3.3.2 Results

The results of the tests in pilot and full-size holes suggest that the average hydraulic conductivity of the rock adjacent to Holes 1 and 2 is on the order of E-8 m/s from 1.5 to 3 m depth, which is about 2 orders of magnitude higher than the average bulk conductivity (9.4E-11 to E-10 m/s) derived from the preceding Macropermeability Test in the drift [9]. The bulk measurements in the latter experiment could not be used for evaluating differences in conductivity in different parts of the drift but a later simpler type of ”ventilation test” showed that the inflow into the inner, 11 m long test section was 13 ml per minute, which was approximately 1/3 of the inflow in the 33 m long drift in which the Macropermeability test had been conducted [1]. The average inflow per meter length was hence about the same along the entire test drift. The frequences of major fractures was also similar along the drift.

The fact that the average bulk conductivity of the rock mass is not higher where the ”wet” holes No 1 and 2 are located is explained by the different orientations of the major fractures. Thus, only the ”wet” holes No 1, 2 and 5 are intersected by water-bearing fractures (blue in Figures 3-1 to 3-3), that are oriented W/E and NW/SE. This coincides with the direction of the major principal stress which yields low tangential pressure in the regions where the fractures intersect the holes. It is hence logical that no major fractures with this orientation intersect the ”dry” holes No 3, 4 and 6.

While it is hardly relevant to derive an average hydraulic conductivity for the near-field rock surrounding the holes with discrete water-bearing fractures it may be so for the rock surrounding holes No 3, 4 and 6. For this rock it would be reasonable to use the bulk conductivity figure E-10 m/s derived from the Macropermeability Test, although it is believed that the stochastic variation implies a variation in bulk conductivity corresponding to the interval E-11 to E-10 m/s.

4 WATER UPTAKE BY THE BUFFER CLAY

4.1 Test program

The Buffer Mass Test comprised heating of the respective clay columns according to the schedule in Table 4.1.

Table 4-1. Test program of the BMT [2].

Hole No	Heater power, W	Start	Stop	Heating time, months
1	600 1400/1800	Oct 5, 1981 March 20, 1984	March 20, 1984 Feb 1, 1985	Ca 30 Ca 10
2	600	Oct 7, 1981	Nov 14, 1984	Ca 37
3	600 1200 1800	Jan 20, 1982 June 13, 1983 Jan 17, 1984	April 12, 1983 Jan 17, 1984 May 21, 1984	Ca 15 Ca 7 Ca 4
4	600	Jan 20, 1982	Dec 1, 1983	Ca 22
5	600	March 24, 1982	June 7,1984	Ca 27
6	600	March 24, 1982	April 6, 1984	Ca 25

4.2 Buffer clay constitution

The buffer consisted of precompacted blocks of MX-80 clay powder. There was a difference in water content between different powder deliveries, w=10 % and w=13 %, which gave a density of 2070 – 2110 kg/m^3 of the dryer powder and 2090 – 2140 kg/m^3 of the wetter one. In order to reach the same net density, the dryer blocks were placed in holes where very little water flowed in because this made it possible to fill the about 3 cm wide gap at the walls with bentonite powder with an estimated density of 1200 kg/m^3. The wetter blocks were given a slightly larger diameter and they were used in the holes where water flowed in at a rate that would have caused difficulties in filling something into the 1 cm wide gap. The net density after complete water saturation should be the same in all the holes.

Different conditions prevailed with respect to water migration from the rock to the buffer. Thus in the ”wet” holes water filled the gap to the rock rather quickly, causing early hydration and expansion of the blocks, while wetting of the loose powder –initially by absorbing water from the moist air - preceded hydration of the dense blocks. Later laboratory studies by Clay Technology AB indicated that the powder in the ”dry” holes is not likely to have retarded the hydration of the blocks.

Backfill of a mixture of bentonite and sand was applied on top of the buffer columns and since its density had to be rather low because of the difficulty in compacting the material with all the cables passing through it, the swelling pressure exerted by the upward expanding blocks gave a drop in block density. This effect was not noticed below mid-height of the heaters, which set a limit to the extension of the investigation.

4.3 Measurement of water content

4.3.1 Principle

The water content was determined at the termination of the respective tests in conjunction with layer-wise extraction of clay samples from the holes parallel to dismantling the heaters. The handling and laboratory treatment of the samples were made so that practically no change in water content could take place. More than 100 samples per 15 cm level were investigated and the data used for plotting ”iso-moisture” graphs. In order to get results that are compatible with the rock structure models and that are representative of the part of the buffer where mainly radial displacement had taken place and where the heater temperature was almost the same over a vertical distance of at least a few decimeters, only the parts of the buffer columns that are defined in Figure 4-1 were used, namely:

1. The part extending from about 1.5 to 2.0 m below the floor (”Upper part”). In some holes the variation in water content changed sufficiently much to divide this part in two halves.

2. The part below the heaters (”Lower part”).

4.3.2 Plottings

The buffer tests in Holes 1 and 2 lasted for 3-4 years and led to practically complete water saturation. They are hence of limited interest for evaluating early wetting stages and are not referred to in this report.

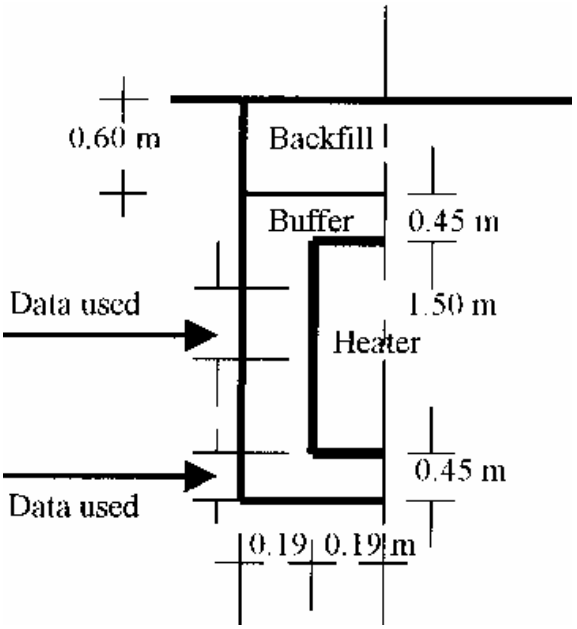

Figure 4-1. *Schematic picture of the geometry of the heater holes (not to scale). Data for the central annuli, representing the hottest parts of the buffer, were used as well as data for the buffer below the base area of the heaters (lowest 0.45 m part).*

The ”iso-moisture” curves at all levels were almost perfectly concentric, which demonstrates that the water that had entered the MX-80 buffer clay had been distributed very uniformly in tangential direction. This is illustrated in Figure 4-2 for Hole 3 in a test with 600 W power.

With the ”iso-moisture” curves as a basis water content profiles could be constructed and they are the ones that were plotted for evaluation with respect to the distribution of the water content as a function of the distance from the heaters and with respect to their shape.

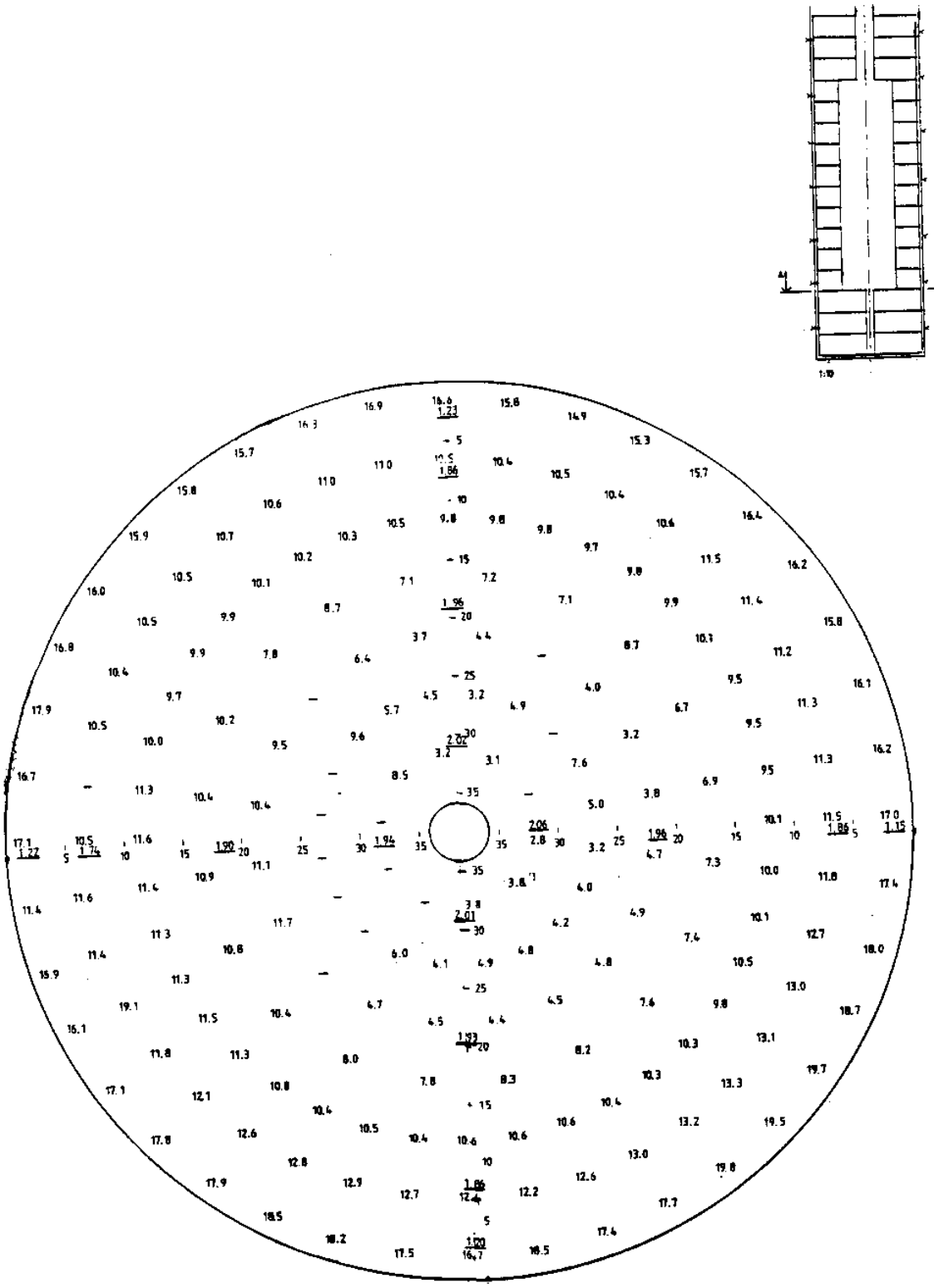

Figure 4-2. *Water content distribution across a horizontal section (A) at the lower end of the heater in Hole 3 (600 W). Very low single values in the interior are due to fissuring of the clay.*

4.3.3 Water content profiles

The distribution of the water content as a function of the distance from the heater surface is shown in Figures 4-3 to 4-7. The plotted data are averages for each zone.

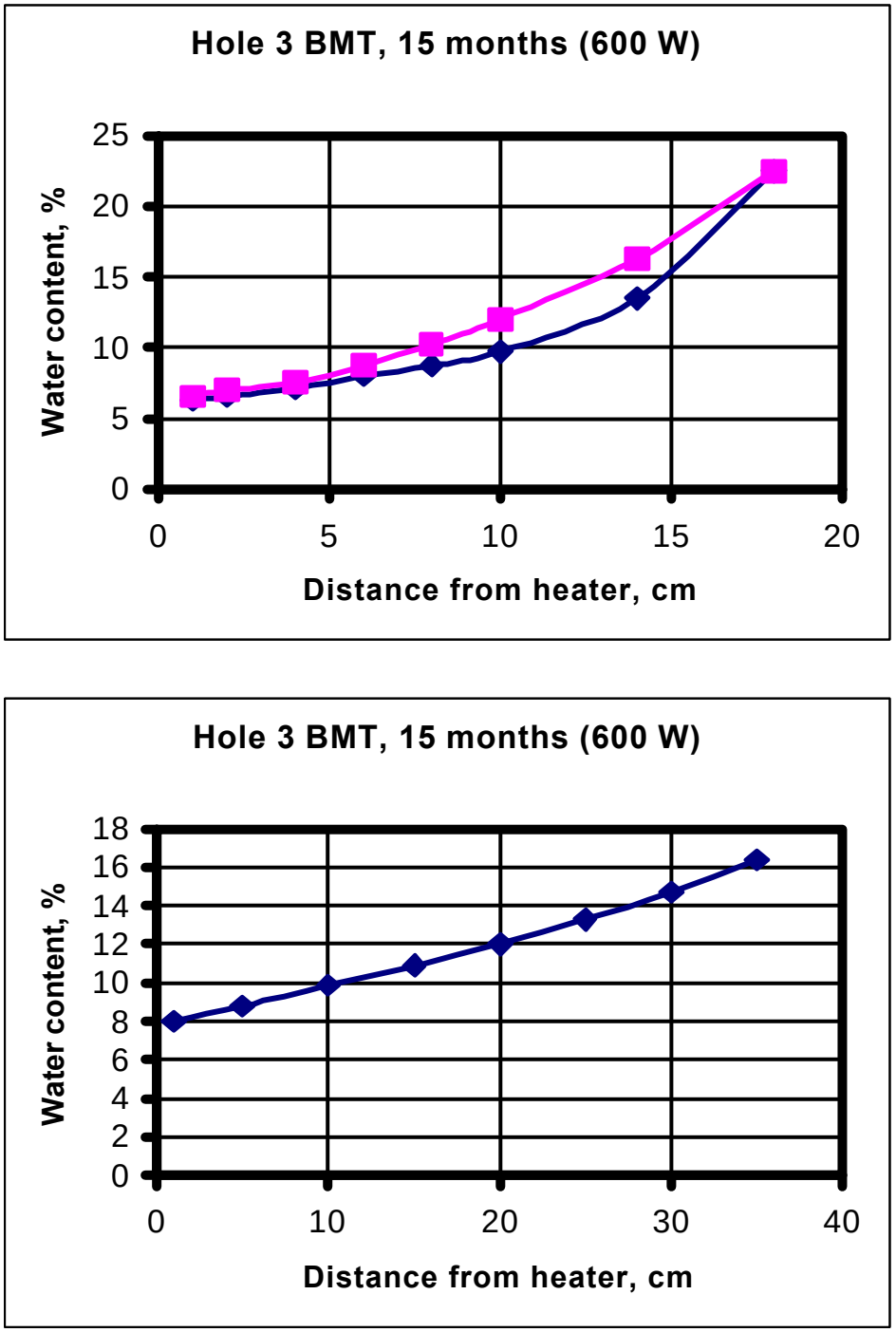

Figure 4-3. *Water content distribution in Hole 3 at termination after 15 months. Upper diagram: Lower curve represents the interval 1.80-2.05 m from the floor, while the upper curve represents the interval 1.50-1.80 m from the floor, both representing different radial distances from the vertical heater wall. Lower diagram: Water content below the heater, data representing different vertical distances from the horizontal heater base. The hole was subsequently used for a second test with new material heated to 1200-1800 W power.*

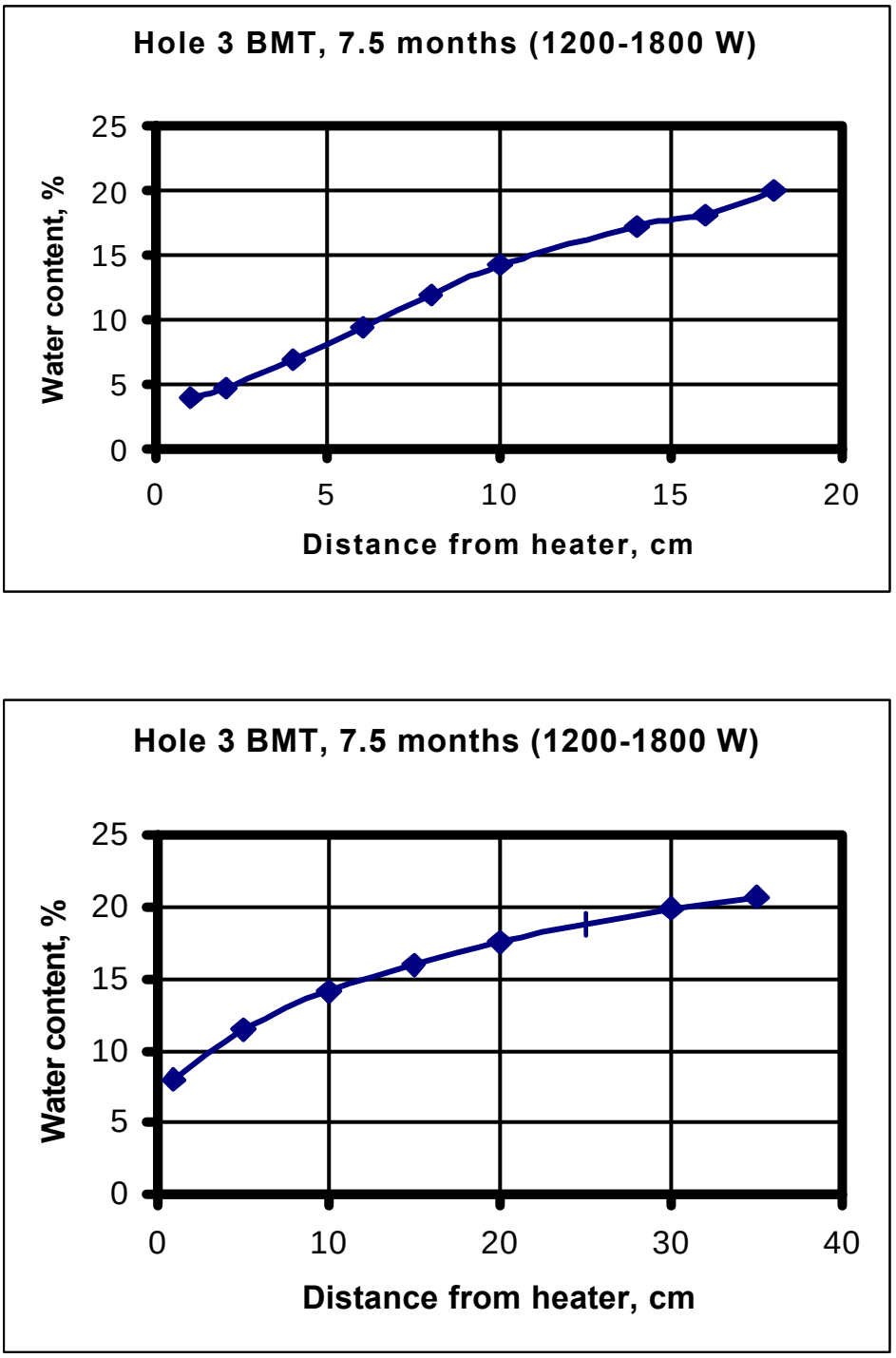

Figure 4-4. *Water content distribution in Hole 3 at termination of the high-power test 7.5 months after start (second test in Hole 3). Upper diagram: Water content distribution for the interval 1.50-2.05 m from the floor, data representing different radial distances from the vertical heater wall. Lower diagram: Water content below the heater, data representing different vertical distances from the horizontal heater base.*

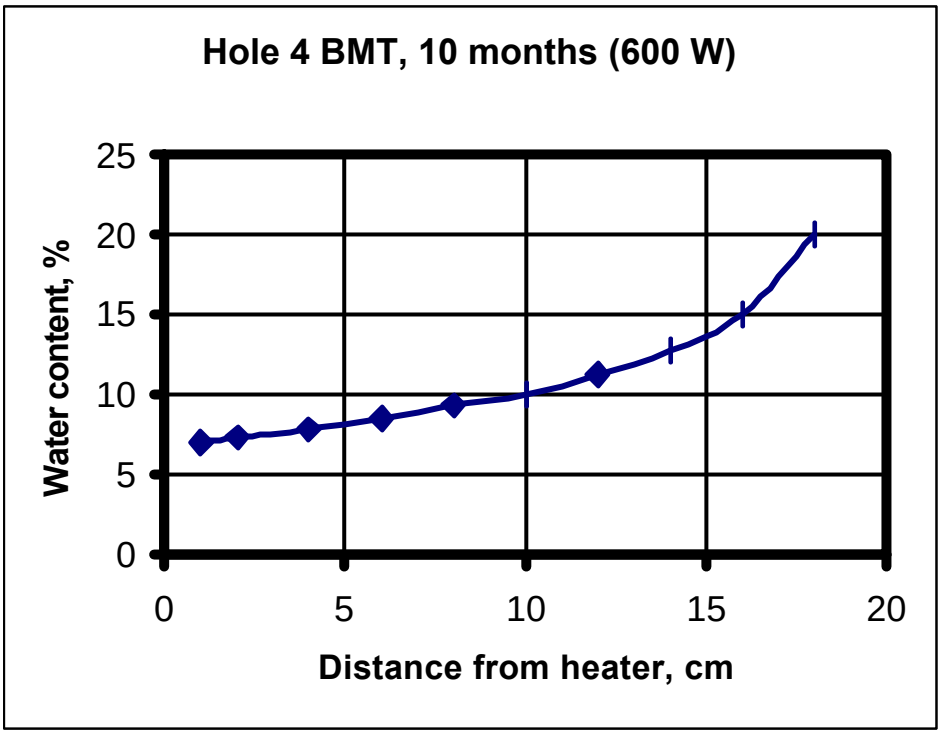

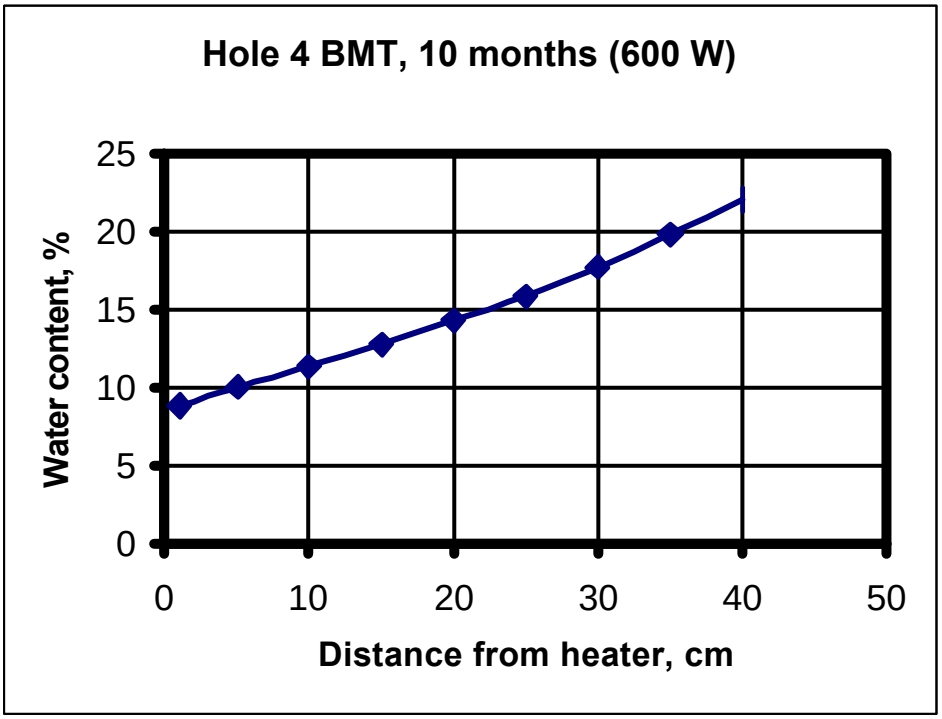

Figure 4-5. *Water content distribution in Hole 4 at termination after 10 months. Upper diagram: Water content distribution for the interval 1.50-2.05 m from the floor, data representing different radial distances from the vertical heater wall. Lower diagram: Water content below the heater, data representing different vertical distances from the horizontal heater base.*

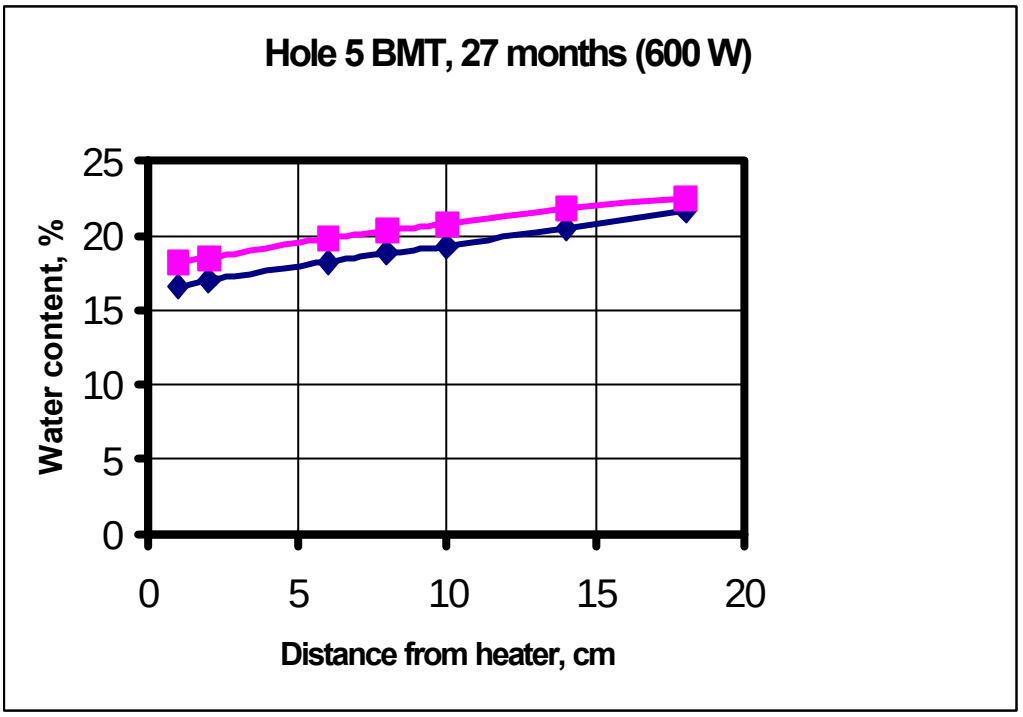

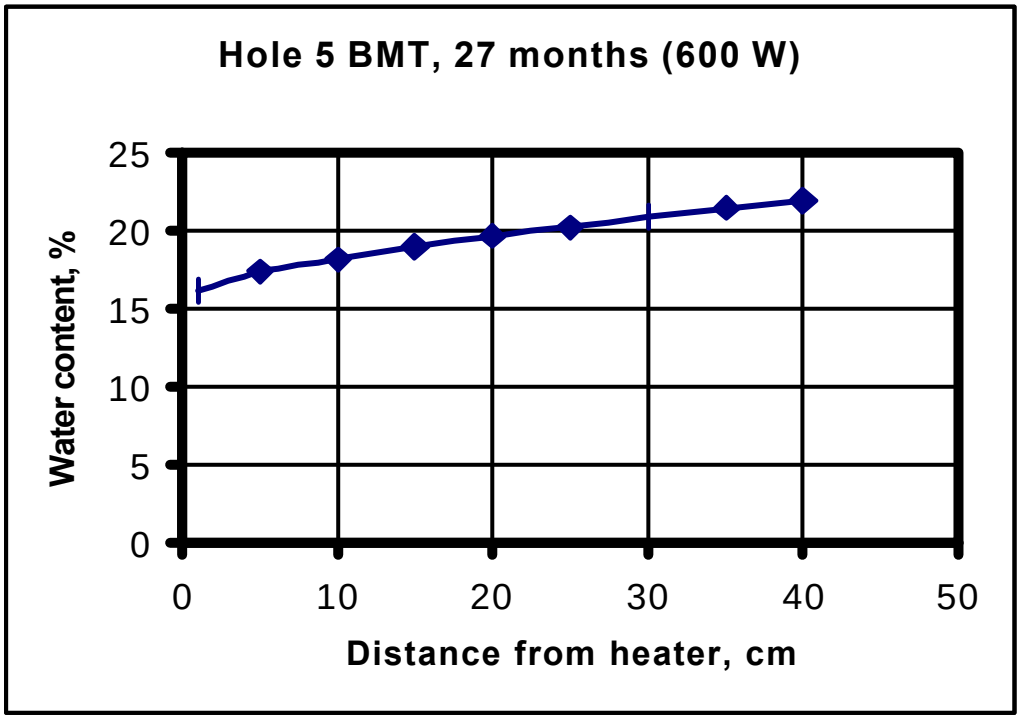

Figure 4-6. *Water content distribution in Hole 5 at termination after 27 months. Upper diagram: Lower curve represents the interval 1.80-2.05 m from the floor, while upper curve represents the interval 1.50-1.80 m from the floor, both give data representing different radial distances from the vertical heater wall. Lower diagram: Water content below the heater, data representing different vertical distances from the horizontal heater base.*

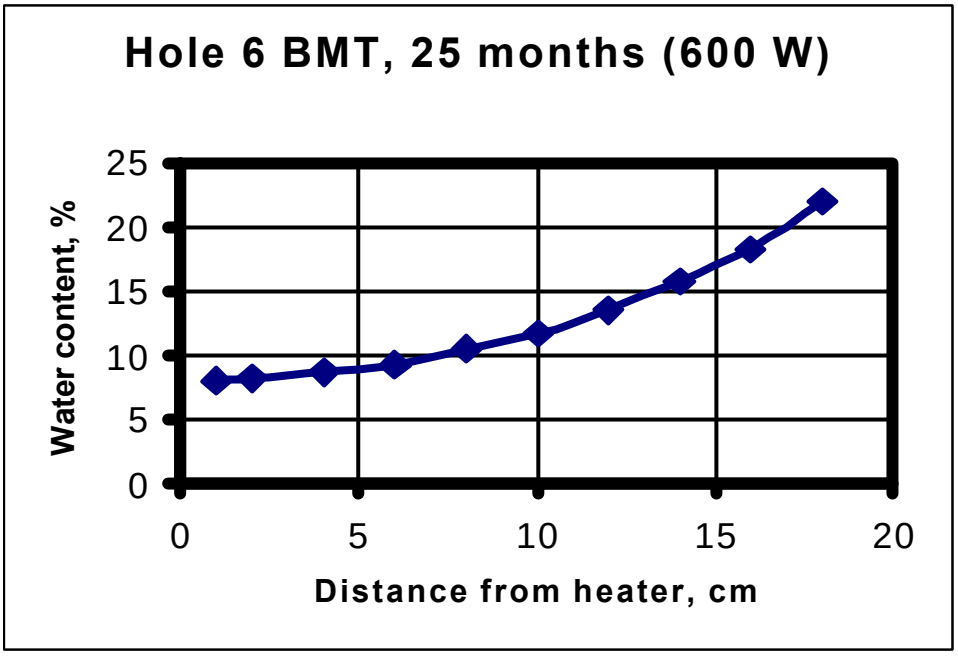

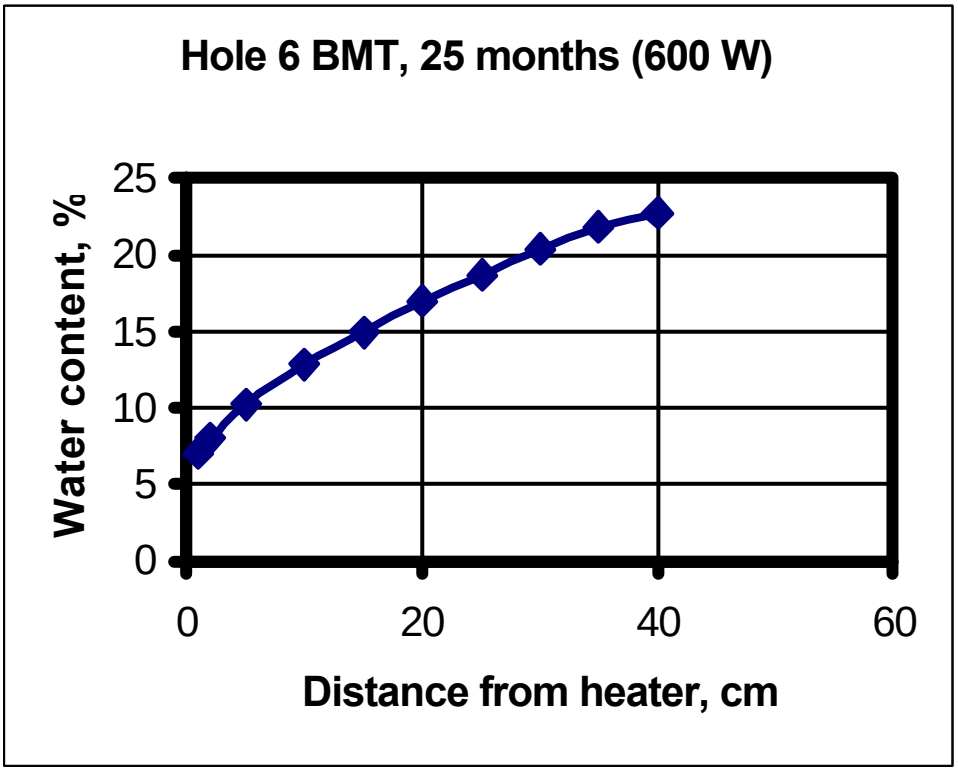

Figure 4-7. *Water content distribution in Hole 6 at termination after 25 months. Upper diagram: Water content distribution for the interval 1.50-2.05 m from the floor, data representing different radial distances from the vertical heater wall. Lower diagram: Water content below the heater, data representing different vertical distances from the horizontal heater base.*

Table 4-2 provides a compilation of the exact positions of the sampled parts yielding the distributions in Figures 4-3 to 4-7.

Table 4-2. Parts from which data were collected.

Hole No	Power, W	Initial water content, %	Time, months	Vertical extension at mid-height from the floor of the drift, m	Annulus below heater, radial distance from rock, m
3	600	10	15	1.50-1.80* 1.80-2.05	0.19-0.30
3	1400-1800	10	7.5	1.50-2.05	0.19-0.30
4	600	10	10	1.50-2.05	0.19-0.30
5	600	13	27	1.50-1.80* 1.80-2.05	0.19-0.30
6	600	10	25	1.50-2.05	0.19-0.30

* Two intervals were investigated because of obvious differences in water content.

The interpretation of the different evolution of the hydration will be made in conjunction with evaluation of the swelling pressure growth, which is reported in the following chapter.

5 EVOLUTION OF SWELLING PRESSURE IN THE BUFFER CLAY

5.1 General

The development of the swelling pressure with special respect to variations along the periphery both tangentially and axially in the buffer clay is directly related to the water uptake and reported in this chapter.

5.2 Plottings

The recorded swelling pressures, representing the average of pressures given by two diagonally placed cells, are plotted in Figures 5-1 to 5-7. ”Serie 1” in the graphs represents mid-height heater and ”Serie 2” the lower part (cf. Figure 4-1 and Table 4-2).

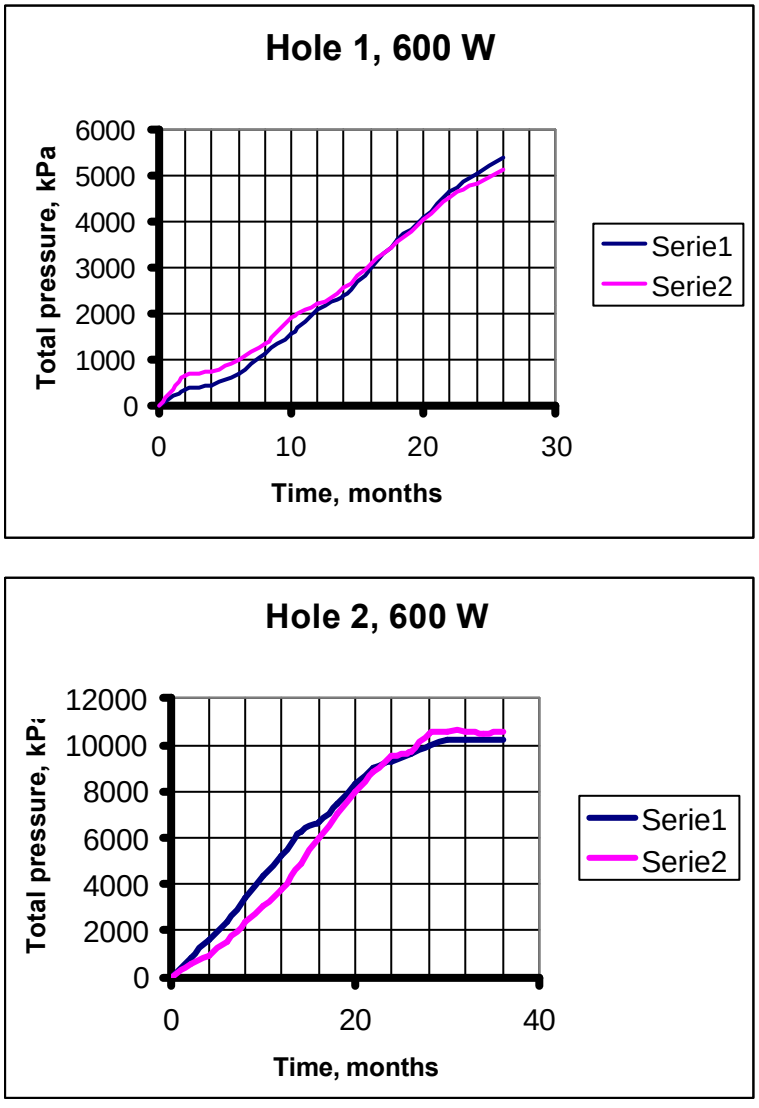

Figure 5-1. *Evolution of swelling pressure in Holes 1 and 2. Almost complete water saturation with build-up of full pressure occurred in Hole 2. Series 1 and 2 were similar.*

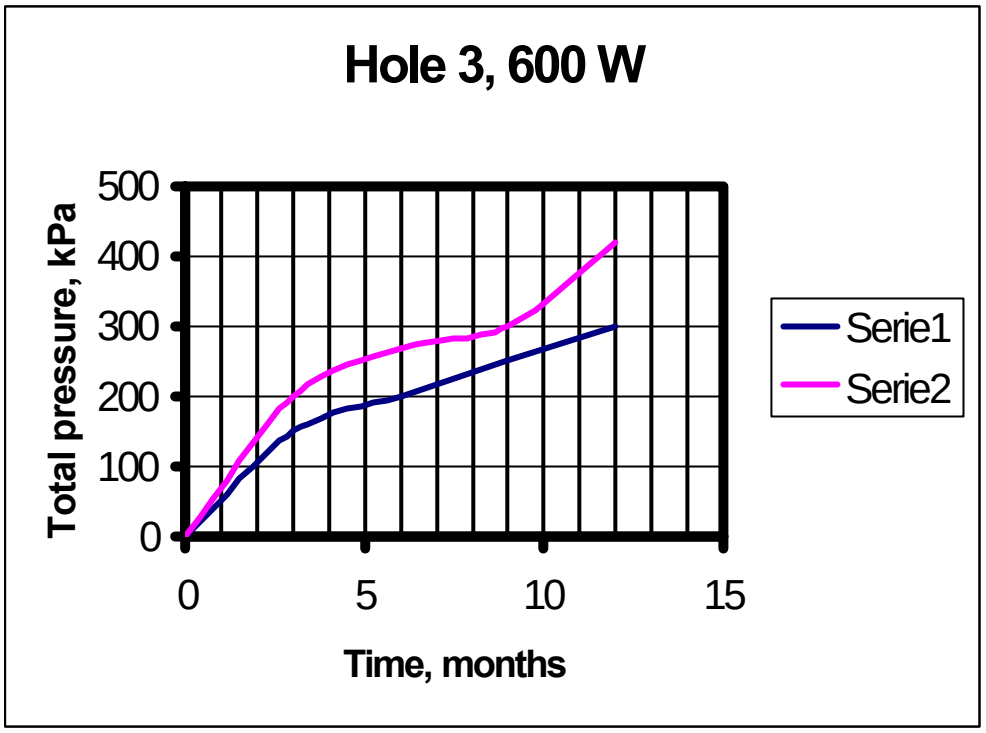

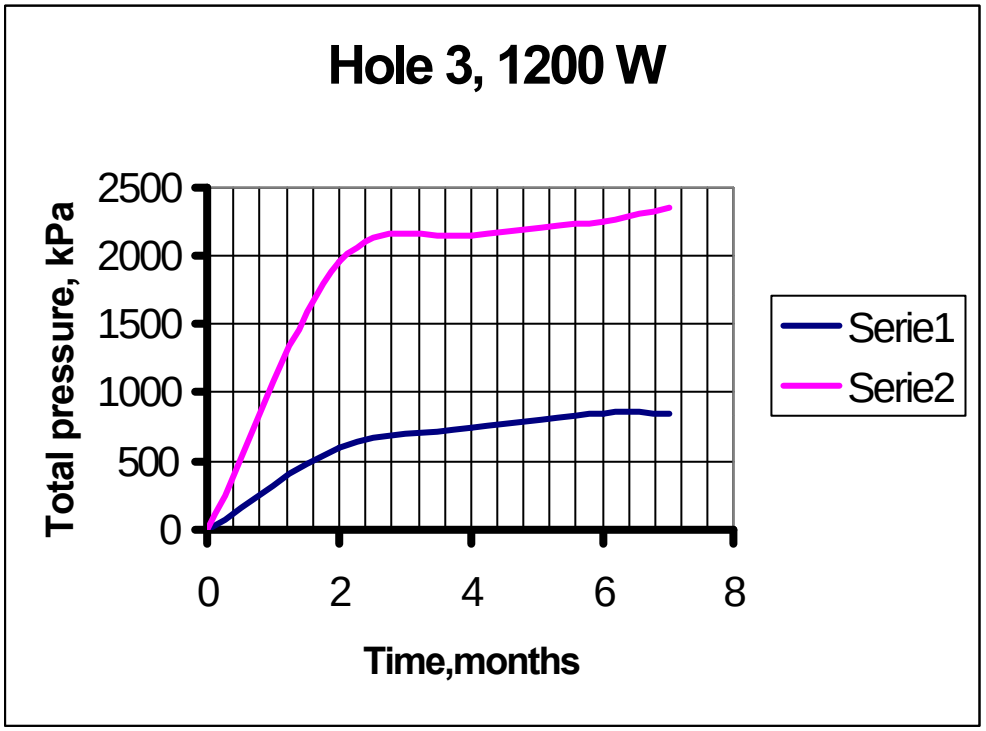

Figure 5-2. *Evolution of swelling pressure in Hole 3. Notice that the swelling pressure grew quicker and reached higher values in the latest test with 1200 W despite the desiccation caused by the significantly higher temperature. The lower part of the buffer(Serie 2) matured more rapidly than the mid part in both tests, especially in the high-power test.*

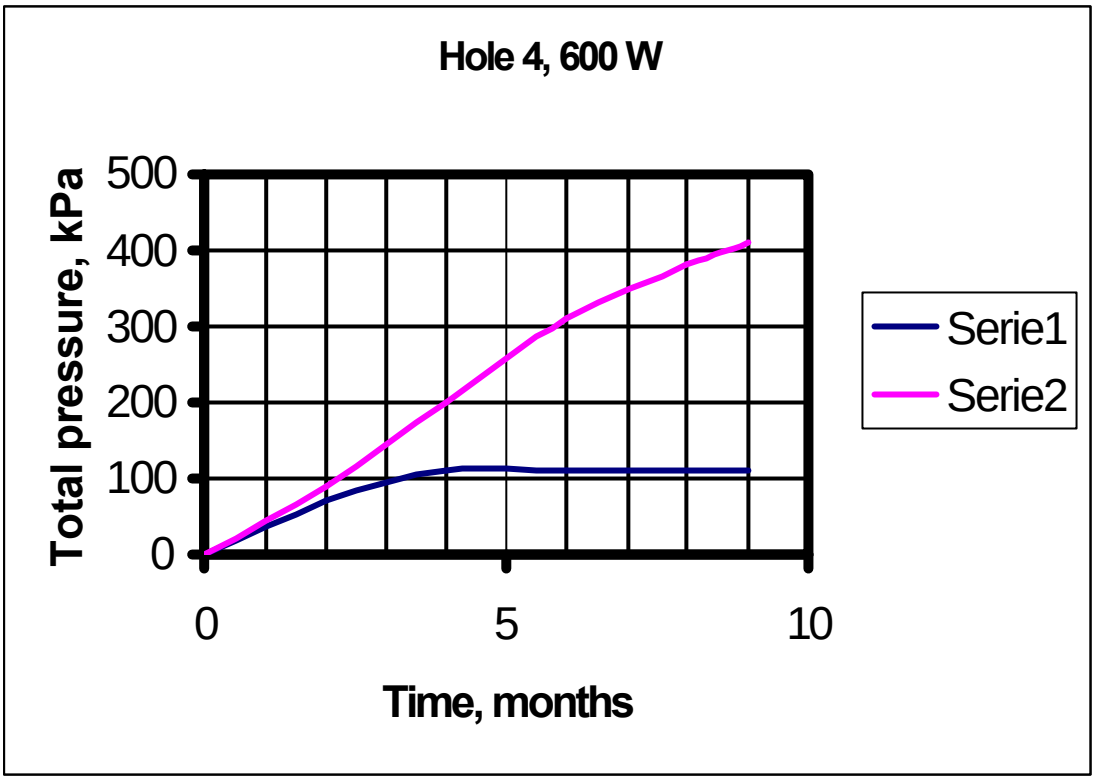

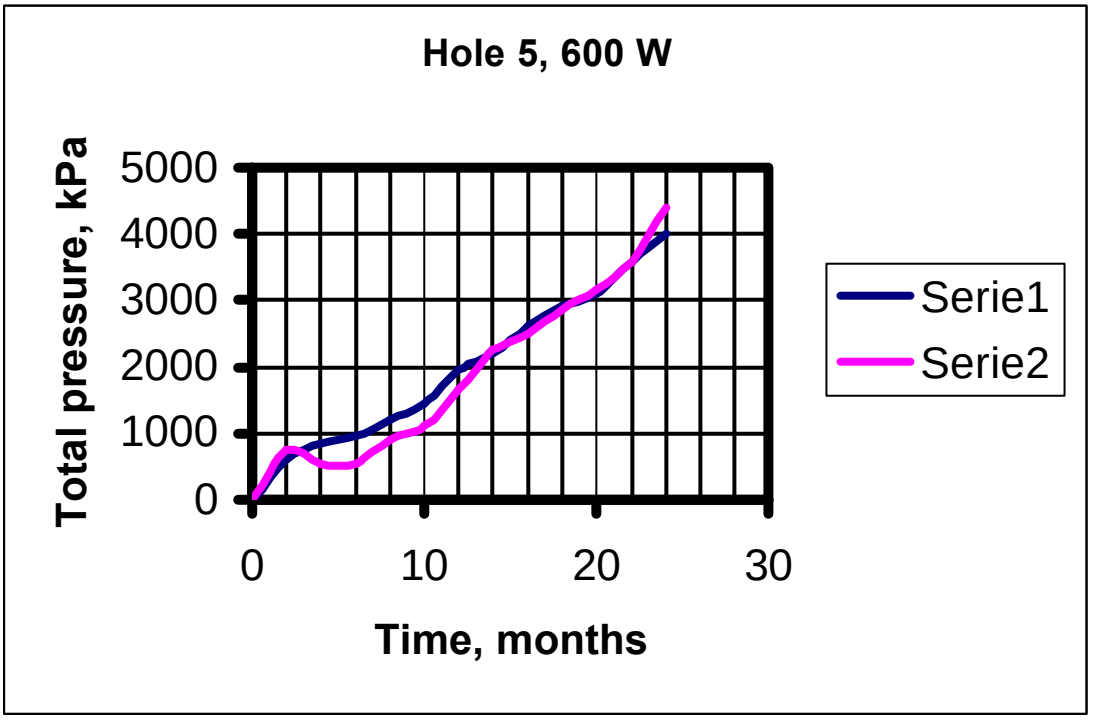

Figure 5-3. *Evolution of swelling pressure in Holes 4 and 5. Notice that the swelling pressure in Hole 5 grew approximately in the same way as in Hole 1. In Hole 4 the buffer at the lower end of the heater (Serie 2) matured more quickly than at mid-height of the heater. In Hole 5 the two parts behaved similarly.*

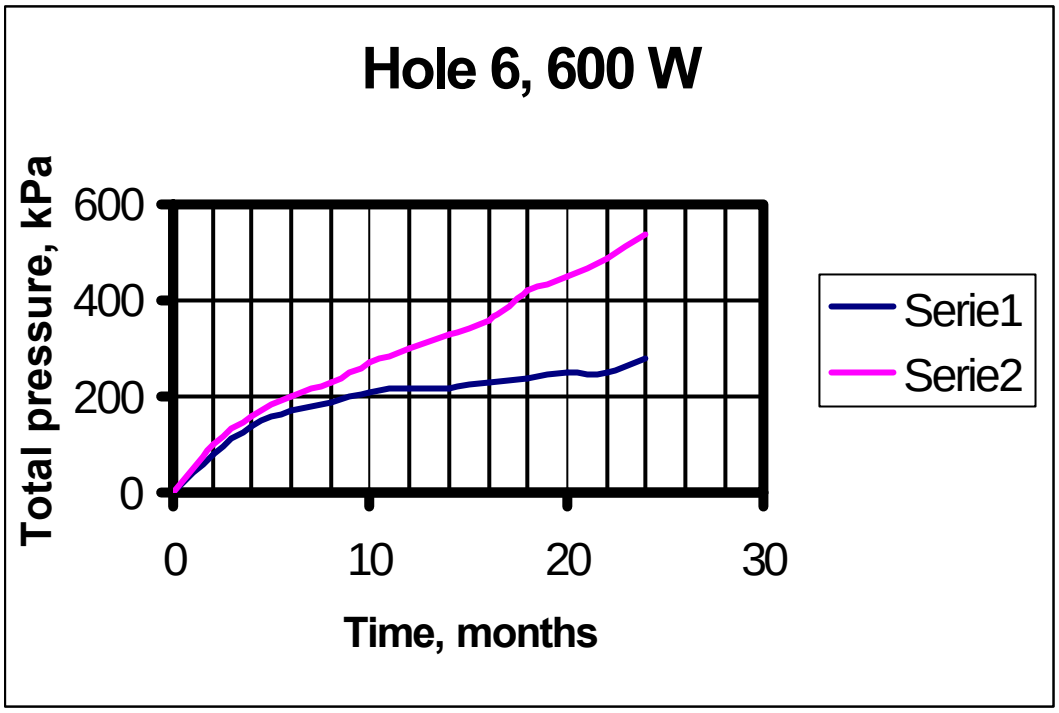

Figure 5-4. *Evolution of swelling pressure in Hole 6. Like in the high-power test in Hole 3 and in the test in Hole 4 the buffer at the lower end of the heater (Serie 2) matured more quickly than at mid-height of the heater.*

The interpretation of the evolution of the build-up of swelling pressures in the experiments is naturally related to the hydration but in particular to a change in hydrological conditions as discussed in the subsequent chapter.

6 CONCLUSIONS RESPECTING THE HYDRATION AND EXPANSION PROCESSES

6.1 Evaluation of the distribution of porewater

Hole 3, 600 W (15 months)

The water content of the buffer from 1.50 to 1.80 m depth below the floor of the drift was higher than in the interval 1.80 to 2.05 m despite the same average temperature conditions (about 80°C close to the heater and a temperature gradient in radial direction of 2.4°C/cm). Drying from the initial water content 10 % took place within 10 cm distance from the heater in the lower part and to 8 cm distance in the upper. There was a net increase in water content in both intervals, 10.8 liters in the upper part and 1.2 liters in the lower one, where the 19 cm thick annulus around the heater had lost 4.5 liters and the outer 4 cm annulus had gained 5.7 liters (cf. Figure 6-1). These findings are compatible with the recorded swelling pressures at the clay/rock contact, i.e. 0.75 MPa in the upper part and 0.35 MPa in the lower part at the end of the test. These pressures were caused by the outermost, saturated or nearly saturated clay which formed arches that left the inner, drier part of the buffer relaxed.

Below the heater the conditions were similar; within 10 cm distance from the base of the heater the water content had dropped somewhat from initially 10 %, while it had increased almost in direct proportion to the distance down to the bottom of the hole. Like in the upper parts of the buffer complete water saturation had occurred only within about 4 cm distance from the rock contact.

A general observation is that very little water had entered the buffer below about 1.80 m depth from the floor of the drift.

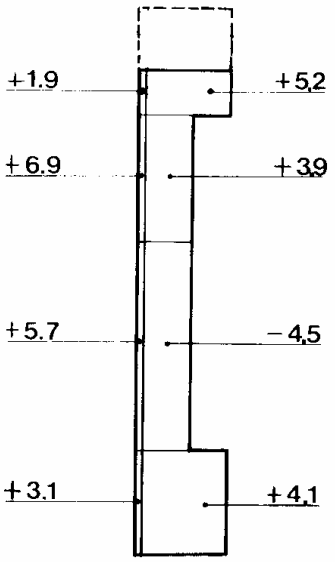

Figure 6-1 *Water uptake (+) and loss (-) in liters in different parts of the buffer column in the 15 months test in Hole 3 (600 W).*

Hole 3, 1200/1800 W (7.5 months)

The water content of the buffer from 1.50 to 2.05 m depth below the floor of the drift had dropped from initially 13 % down to about 4 %, i.e. lower than in the 600 W test within 8 cm distance from the heater. The temperature close to the canister was about 170°C and the temperature gradient in radial direction about 5°C/cm. Drying from the initial water content took place within 8 cm distance from the heater as in the 600 W test and as in this test there was a small net increase in water content. However, the two tests were different with respect to the extension of the part that had got a significant increase in water content as shown in Table 6-1, which shows that despite the more than two times higher temperature and temperature gradient in the case with higher power, more water was absorbed. The table shows that the relative increase in water content from 8 to 15 cm was stronger in the high-power test than within the depth interval 1.80 to 2.05 m in the 600 W test.

Table 6-1. Increase in water content in percent of the intial water content in the two tests in Hole 3. First figure is initial water content, second is recorded after the test. Third figure is the increase in water content in percent of the initial water content.

Power, W	Time, months	8-10 cm from heater	10-12 cm from heater	12-15 cm from heater	15-18 cm from heater	Height interval from the floor of the drift, m
600	15	10/11.5/12	10/13/30	10/17/70	10/18/80	1.50 to 1.80
600	15	Drying	10/11/10	10/12.5/25	10/18/80	1.80 to 2.05
1200/1800	7.5	13/14/7	13/15.5/19	13/17/30	13/18.5/42	1.50 to 2.05*

* No difference between the 1.50-1.80 and 1.80-2.05 m intervals

The swelling pressures at the clay/rock contact increased more rapidly than in the 600 W test. In the first phase of the high-power test the power was kept constant at 1200 W for 7 months and was then increased to 1800 W. The water content distribution determined on extracted clay samples represent the state about 4 months after the power increase to 1800 W. The total pressure at that time was high due to the associated expansion of the porewater. In contrast, the pressure recorded after 7 months is a safe measure of the swelling pressure and it was found to be about 0.3 MPa at mid-height of the heater as in the 600 W test.

Below the heater the conditions were similar to those higher up; within 10 cm distance from the base of the heater the water content had dropped somewhat from initially 10 %, while it had increased almost in direct proportion to the distance down to the bottom of the hole. Like in the upper parts of the buffer complete water saturation had occurred only within about 4 cm distance from the rock contact.

A general observation is that somewhat more water had entered the buffer below about 1.80 m depth from the floor of the drift than in the 600 W test.

Hole 4, 600 W (10 months)

The water content distribution in the buffer from 1.50 to 2.05 m depth below the floor of the drift was practically identical to that of the depth interval 1.80 to 2.05 m in 600 W test in Hole 3. It is concluded that very little water, about 2 liters, had entered from the rock in this 10 months long test. However, below the heater somewhat more water had entered the buffer as concluded from Table 6-2.

Table 6-2. Increase in water content in percent of the intial water content below the heaters in the tests in Hole 3 and Hole 4. First figure is initial water content, second is recorded after the test. Third figure is the increase in water content in percent of the initial water content.

Hole (600 W)	Time, months	5-10 cm from heater	10-20 cm from heater	20-30 cm from heater	30-40 cm from heater
3	15	10/9/drying	10/12/20	10/13/30	10/16/60
4	10	10/11/10	10/12.5/25	10/16/60	10/20/100

Hole 5, 600 W (27 months)

The water content of the buffer from 1.50 to 1.80 m depth below the floor of the drift was slightly higher than in the interval 1.80 to 2.05 m despite the same average temperature conditions (about 80°C close to the heater and a temperature gradient in radial direction of 2.4°C/cm). At the time of termination the entire buffer column had undergone wetting and in the upper part the degree of saturation was about 75-80 % within 10 cm distance from the heater and 80-95 % within 10 to19 cm distance. In the lower part the corresponding figures were 70 and 85 %, respectively. These findings are compatible with the recorded swelling pressures at the clay/rock contact, 3.7-4.2 MPa. The water content ranged between 18 and 22 % in the upper part and between 17 and 22 % in the lower part, which means that the relative increase in water content was on the order of 30 to 70 %.

It is clear from the recording of swelling pressures that the wetting took place almost proportionally to time after test start. It is hence believed that the increase in water content from the initial 13 % can have been about 50 % of the final values. Thus, after 15 months the water content in the inner 10 cm annulus is expected to have been 15-16 % and 17-18 % in the outer annulus with 9 cm radial thickness. These data illustrate that the wetting was much stronger in this test than in the tests in Hole 3 and hence that the hydrological or wetting mechanisms were different in Holes 3 and 5.

Below the heater the conditions were similar; within 10 cm distance from the base of the heater the water content had increased from 13 to about 17 % and to 19 % in the interval 10-20 cm. Furter down the water content had increased to more than 20 % and the clay was almost completely saturated at 40 cm distance from the heater. The wetting of the buffer below the heater was hence much stronger than in the tests in Hole 3 and also considerably stronger than in the test in Hole 4.

Hole 6, 600 W (25 months)

The water content distribution was similar to that of the upper part of the buffer in the 15 months long test with 600 W power in Hole 3, the temperature conditions of which were practically identical to those in the tests in Hole 6. Drying from the initial water content 10 % took place within 8 cm distance from the heater and there was an increase in water content to 12 to 17 % between 10 to 15 cm distance from the heater. In the interval 15 to 18 cm the water content had risen to 17 to 22 %. There was a tendency for the water content to be slightly higher in the upper part of the investigated buffer column.

Like for the 600 W test in Hole 3 the recorded swelling pressure at the clay/rock contact was 0.8 MPa in the upper part and about 0.3 MPa in the lower part at the end of the test, hence indicating a somewhat higher water content in the upper part.

Below the heater the conditions were very similar to those in the 1200/1800 W test in Hole 3. Within 5 cm distance from the base of the heater the water content had dropped somewhat from initially 10 %, while it had increased almost in direct proportion to the distance down to the bottom of the hole. Like in the upper parts of the buffer complete water saturation had occurred only within about 4 cm distance from the rock contact.

6.2 Major observations respecting the wetting process

It is obvious that the rate of wetting was similar and slow in the experiments with 600 W power in Holes 3, 4 and 6, while it was more rapid in Hole 5 and even quicker in Holes 1 and 2 as indicated by Figure 5-1, which shows that a stable pressure of around 10 MPa was built up after about 30 months at mid-height of the heater. This diagram shows that the pressure was about 4 MPa after 10 months, 6 MPa after 15 months and 8 MPa after around 20 months.

An important observation as to the water content at mid-height of the heaters was that the wetting curves in all the 600 W tests except for the "wet" hole No 5, were diffusion-like, i.e. with an upward concave shape showing a non-linear, successive drop in concentration (water content) with increasing distance from the rock (Figure 6-2), while below the heaters the drop in concentration was practically proportional to the distance from the rock. This suggests that the hydration mechanisms were somewhat different such that flow under pressure contributed more to the wetting of the buffer at the base, yielding a water content profile of the type "moving front". For the 1200-1800 W test the latter type of curve was obtained both at mid-height of the heater and below it and this shape was obvious also in the test in Hole 5.

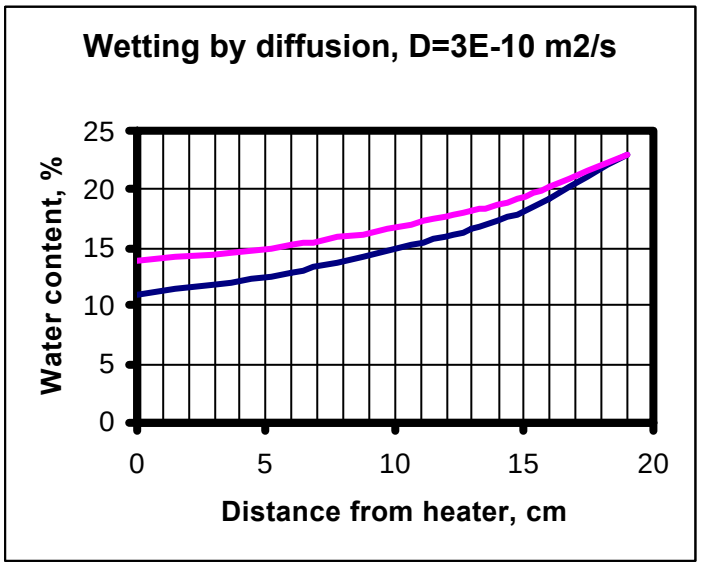

Figure 6-2. *Example of calculation of water content distribution using BMT material data but omitting thermal effects. Upper curve: Condition after 15 months. Lower curve: Condition after 9 months.*

One can draw three major conclusions from the examination of the water content in the buffer clay:

1. The holes with insignificant water inflow before application of the buffer clay, i.e. Holes 3, 4 and 6, gave slow but successive wetting of the clay. Extrapolation suggests that it would have taken more than ten years to reach a high degree of water saturation under the prevailing piezometric conditions. The holes with significant water inflow, i.e. Holes 1 and 2, gave almost complete saturation of the buffer clay in about 3 years while this state is believed to have required about 6 years for the buffer in Hole 5, which had an intermediate rate of inflow of water.

   The conclusion from this is that the migration of water to the deposition holes as recorded before applying buffer clay in the holes largely controls the rate of water saturation of the buffer.

2. In Hole 3 the rate of wetting was different in two consecutive tests. The first test with 600 W power gave slower wetting than in the subsequent test with 1200/1800 W power. The vapour pressure in the hottest part (about 170°C) of the latter test was on the order of 6 MPa while it was only about 0.5 MPa in the preceding one, and it can be assumed that some dissipation of vapour occurred through the overlying buffer and backfill. Despite this loss of water the wetting of the buffer was faster than in the low-temperature test and this is explained by an increased rock water pressure and flow to Hole 3 that was caused by the increased degree of water saturation of the backfill behind the bulwark that separated Holes 1 and 2 from Hole 3 [2, page 178].

   The increased flow to Hole 3 is believed to have been caused by a higher water pressure giving access to more water in the high-power test and hence yielding quicker wetting of the buffer.

3. The shapes of the water distribution curves appear to be related to different mechanisms of water uptake in the buffer: Where the rock did not supply much water for saturation of the buffer, plotting of the water content of the buffer of the type applied in the present chapter yields ”diffusion”-type curves, while where the rock gave off much water the curves are more of the type ”moving wetting front”. This does not imply that water flowed uniformly into the buffer; it may be that where the water pressure was sufficient to penetrate into joints between blocks or along cables and instruments and further into cracks in the dryer zone near the heaters. Such locally absorbed water was then redistributed vertically as well as radially in a complex pattern that was largely controlled by the thermal gradient.

   The different shapes of the water content distribution curves indicate that there were two wetting mechanisms: 1) diffusion of water from the rock where the water pressure in the rock was low and the rock only discharged little water, and 2) flow where the water pressure was higher and probably caused penetration into the buffer through joints and cables.

6.3 Influence of rock excavation and disturbance on the hydration of the buffer

6.3.1 General

Three processes combine to change the hydraulic conductivity of the rock adjacent to large-diameter holes like those in the BMT experiment:

- Mechanical damage by the cutters
- Changes in rock stresses that affect the conductivity of discrete water-bearing fractures
- Strain of the rock by which high-order rock discontinuities that were previously not hydraulically active to become active

Excavation damage

The large holes were core-drilled which gave very little rock disturbance; it is estimated to have caused only fine-fissuring to a few millimeters depth but the matter has not been investigated in detail. This is in contrast with the influence of TBM boring, which causes damage of the grain structure to 10-20 mm depth (Figure 6-3). An example of the type of damage that takes place is shown in Figure 6-4. Determination of the hydraulic conductivity of small samples extracted from the walls of TBM tunnels has shown that it is two orders of magnitude higher than that of the unfractured crystal matrix within 5 mm distance from the rock wall.

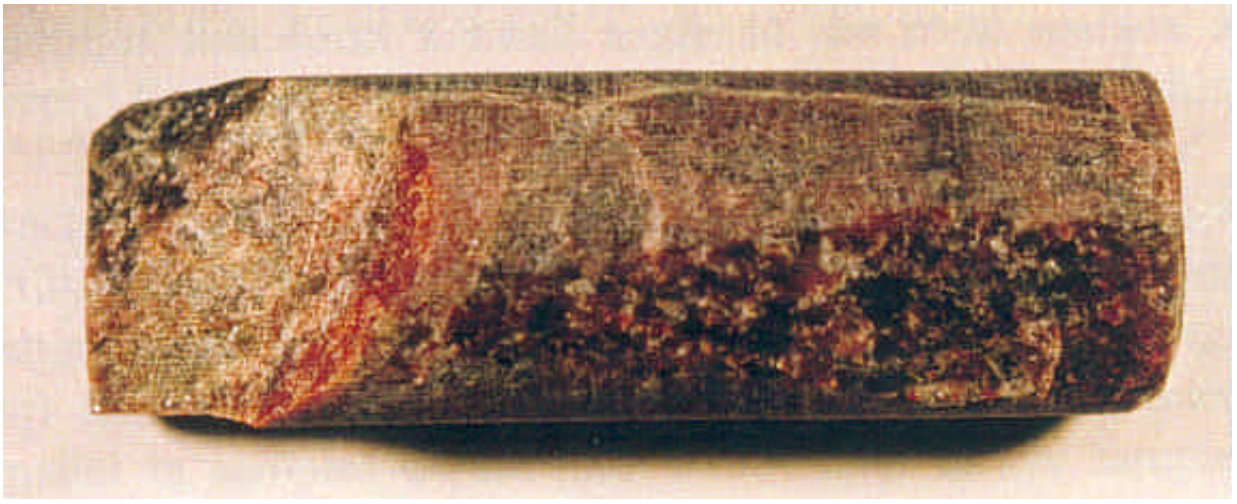

Figure 6-3. *Example of fracturing in the boring-disturbed wall of a 5 m diameter TBM drift in granite (AEspoe). The core has a diameter of 10 mm and a length of about 16 mm. The coring was made perpendicularly to the wall surface. Notice the axial fissures and the ones parallel to the inclined fracture surface.*

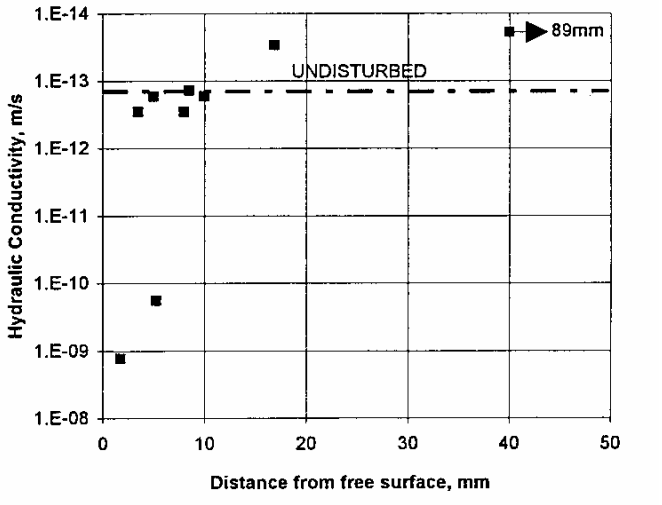

Figure 6-4. *Results from determination of the hydraulic conductivity of small undisturbed samples of shallow rock extracted by boring from the wall of a TBM-tunnel in AEspoe granite [11]. The testing was made by use of a triaxial cell.*

Recent field determination of the hydraulic conductivity in shallow boreholes at AEspoe has verified that the average hydraulic conductivity of the rock surrounding the TBM tunnel is in the interval E-10 to 5E-10 m/s to a depth of 1 cm from the periphery [12]. These results are compatible with determinations of the porosity, which have shown an obvious increase to 12 mm distance from the walls of big boreholes in tonalite [13].

Boring also erodes preexisting fractures, fissures and voids by which a network of a few millimeters deep scars can be developed as illustrated by Figure 3-5. Assuming them to interact and make up orthogonal patterns of 3 mm deep slots with 1 cm spacing and 100 µm aperture one finds that the most shallow part of the wall may represent an average hydraulic conductivity of as much as E-9 to E-8 m/s.

Changes in normal stress on discrete fractures

The rock stress situation in the blasted BMT drift implied considerable relaxation of the rock stresses down to about 1.5 m below the floor but below this depth there was an impact on the water-bearing fractures. Thus, the original normal pressure on the ones oriented W/E to NW/SE (marked blue in the structure models in Figures 3-1 to 3-3) was somewhat reduced by the creation of the holes while those oriented NE/SW (marked red) were exposed to increased normal pressure. Subhorizontal fractures (marked green) did not undergo significant stress changes. This is a major explanation of the different water-bearing capacity of the differently oriented fractures.

Stress-generated activation of fine discontinuities

In addition to the impact of the altered normal stress on the fracture planes there was probably also an influence of the secondary stresses generated by the creation of the holes that has to do

with scale-dependence of the bulk strength of the rock. Thus, the induced shear stresses within a distance of a few decimeters is believed to have activated finer latent weaknesses, which may thereby become flow paths. The stress-disturbing influence on the immediate surrounding of big holes is illustrated in Figure 6-5, which shows the evolution of plastization around a borehole with 1.5 m diameter in rock with Mohr/Coulombian performance.

The assumed parameter values are taken to represent the mean strength of a rock volume of a few cubic meters while those of an element of an ordinary core sample would be c=10-50 MPa and ϕ=45-60^o. One sees that the upper two examples in the figure indicate local failure along the entire shaft, while the lower example with high strength parameters shows failure only below the drilling head. Such failure cannot result in comprehensive breakage and disintegration of the rock since it is effectively confined but it is believed to result in slight shearing and propagation of weaknesses of 4th and higher orders.

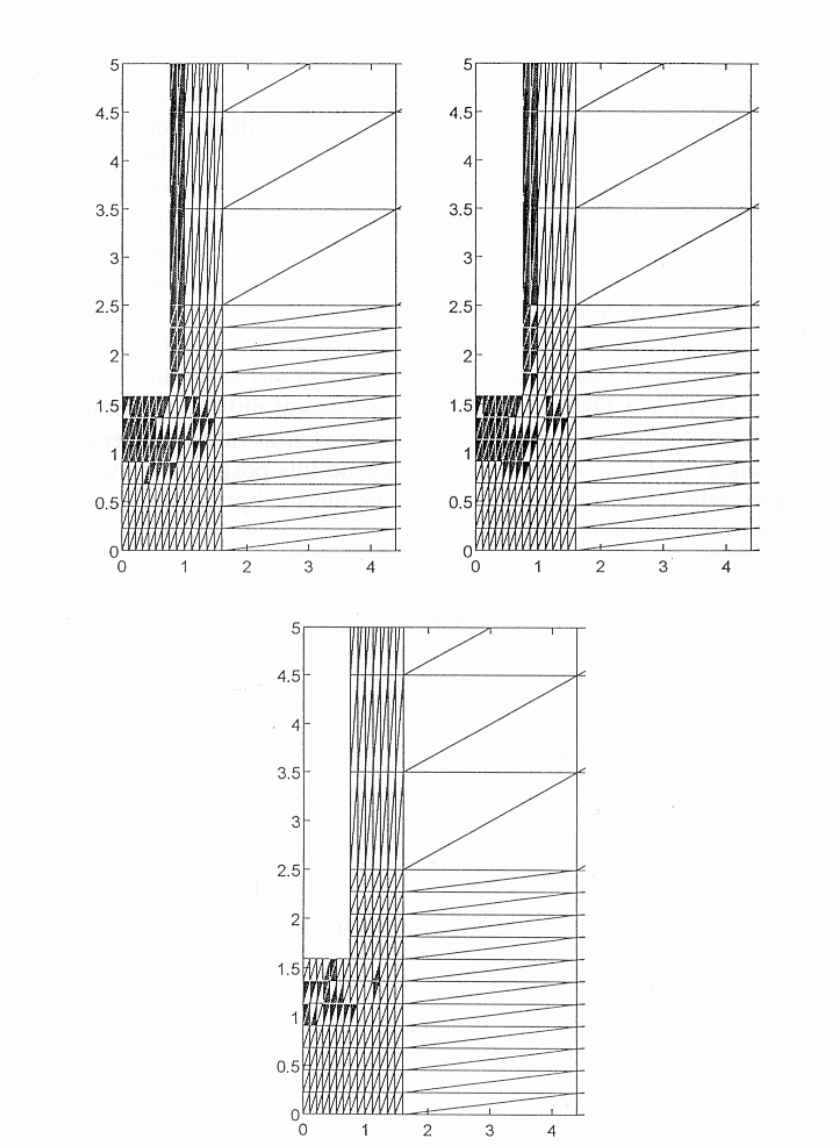

Figure 6-5. *Plastization (black elements) of deep 1.5 m diameter borehole. Upper left: c=0.5 MPa and =30^o. Upper right: c=1 MPa and =30^o. Lower: c=5 MPa and =40^o [6].*

6.3.2 Net effect of the disturbance

As to the contribution to the bulk hydraulic conductivity by the damaging processes one concludes that the most shallow disturbance by mechanical abrasion and erosion of fractures and fissures may lead to a shallow annulus of about 5-10 mm radial thickness with an average hydraulic conductivity of around E-9 to E-8 m/s.

The stress-generated activation of pre-existing less important weaknesses within a few decimeters from the wall of the holes may cause an increase in average hydraulic conductivity that is more difficult to estimate but it seems reasonable to assume that it could correspond to some intermediate value between E-9 m/s and the average value for undisturbed rock as determined in the Macropermeability test, i.e. E-10 m/s. It may extend to a couple of decimeters from the wall of the holes. Outside this region undisturbed conditions are assumed to prevail below about 1.5 m depths from the floor of the drift.

The most important effect of the creation of big holes in stress fields of the type in Stripa rock is that steep water-bearing fractures oriented more or less in the direction of the major principal stress become more transmissive while those oriented in the perpendicular direction become less conductive.

It is proposed that the near-field rock structure of the immediate surrounding of the holes is as shown in Figure 6-6 and the average hydraulic conductivity as summarized in Table 6-3.

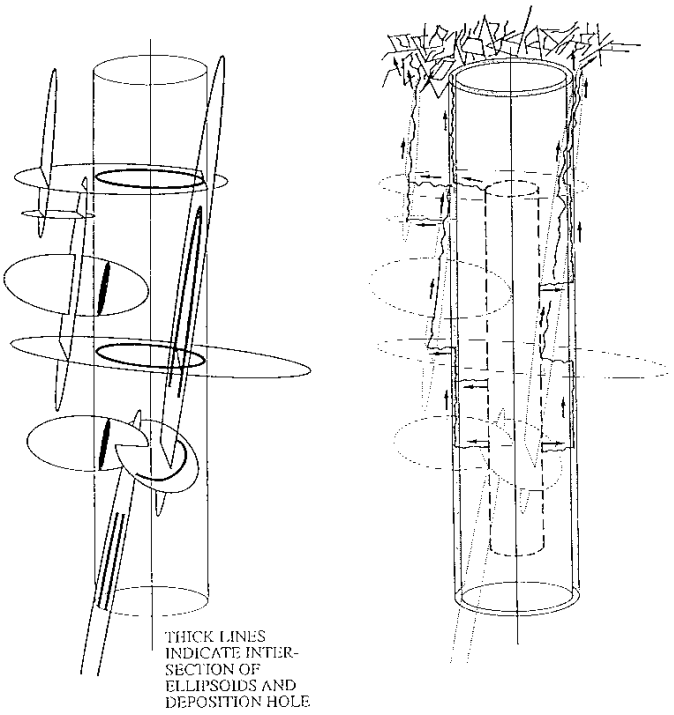

Figure 6-6. *Schematic picture of hydraulically important structural features in the near-field rock. Left: System of interconnected discontinuities with varying water-bearing capacity. Right: Transport paths of gas and radionuclides from leaching canisters up to the floor of blasted tunnel via the continuous boring-disturbed zone [14].*

Table 6-3. Proposed distribution of the hydraulic conductivity in the rock surrounding the BMT heater holes.

Rock zone	Average hydraulic conductivity, m/s
Most shallow 5-10 mm annulus	E-9 to E-8
Second annulus 10-200 mm	E-10 to E-9
Discrete fracture	Unlimited
Undisturbed bulk rock	E-11* to E-10

The stochastic variation in bulk rock conductivity implies that the range also comprises lower values than provided by the Macropermeability test

The data proposed in Table 6-3 suggest that the second annulus with about 200 mm radial thickness is the most important transmissive part of the nearfield.

6.3.3 Proposed near-field rock structure cases

Considering that there may be two zones of disturbance and keeping in mind that discrete significantly water-bearing fractures control the inflow of water to the holes one can define three typical rock structure cases, i.e. those in Figure 6-6. In all the cases there is a shallow mechanically disturbed zone with rather high hydraulic conductivity (black ring in the figure), which is surrounded by a stress-disturbed zone with a somewhat lower conductivity and a radial thickness of a few decimeters outside which there is undisturbed rock. The left case in the figure represents the ”wet” Holes 1, 2 and 5 in the BMT, while the right case may represent the ”dry” Holes 4 and 6. The ”dry” Hole 3 that got more water in because of increased water pressure in the surrundings may correspond to the middle case in which the stress-disturbed zone but not the hole is intersected by a significantly water-bearing fracture.

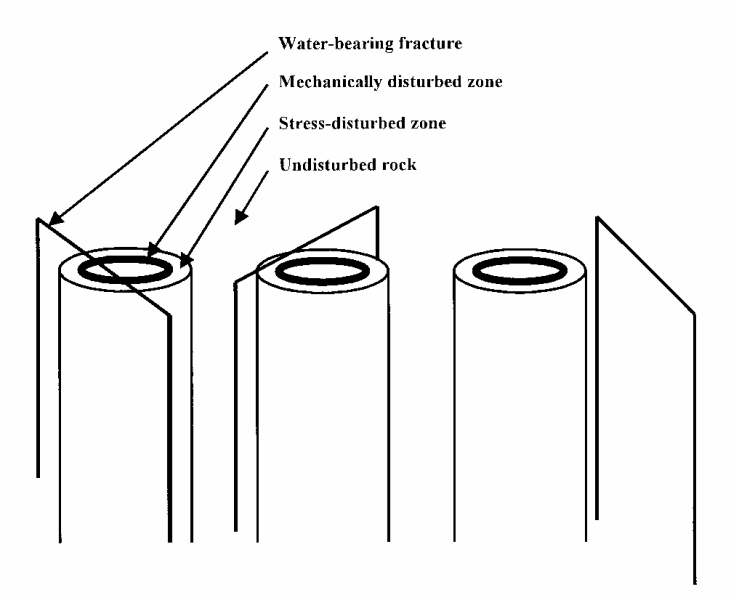

Figure 6-7. *Three rock structure types with different impact on the saturation rate of the buffer. Left: Water-bearing fracture intersecting the hole. Middle: Water-bearing fracture intersecting the disturbed zone. Right: No water-bearing fracture intersecting the hole or disturbed zones.*

7 DISCUSSION AND CONCLUSIONS

7.1 Behavior of the near-field rock around the lower part of the holes

Considering the rock stress situation the rock structure models imply that the W/E- to NW/SE-oriented 4th order discontinuities are the most strongly water-bearing structural features. They are found to intersect only Holes 1, 2 and 5, which also turned out to be the ”wettest” with respect to the saturation rate of the buffer. This indicates that the buffer in a future repository of KBS-3 type will be hydrated in a few years if the deposition holes are intersected by such fractures while it will take decades to get the buffer saturated in holes with no such features. This is with the reservation that high water pressures may affect the buffer saturation rate.

The wetting of the buffer in tangential direction was very uniform and this was also obvious in the ”wet” hole No 5, which is intersected by two effectively water-bearing fractures. Hence, despite the local inflow into this hole there was effective distribution over the entire periphery of entered water. The reason for this seems to be an increased average hydraulic conductivity of the rock and it is possible that there is not only a shallow mechanically damaged EDZ but also a stress-generated zone of disturbance with somewhat higher conductivity than that of undisturbed rock, assisting in distribution and transport of water from discrete water-bearing fractures.

7.2 Major observations with respect to the water saturation

- The rate of wetting was similar and slow in the experiments with 600 W power in Holes 3, 4 and 6, while it was more rapid in Hole 5 and even quicker in Holes 1 and 2. A stable swelling pressure of around 10 MPa was built up after about 30 months at mid-height of the heaters in the latter ”wet” holes.

- The plotted water content curves for mid-height of the heaters in the ”dry” holes and the swelling pressure measurements show a slow but continuous uptake of water from the rock. The curves are diffusion-like, while those representing the buffer below the heaters suggest that flow under pressure contributed more to the wetting of the buffer, probably by pressure-induced penetration through joints, cables and instruments, yielding a water content profile more of the type ”moving front”.

- In one hole (No 3) the rate of wetting was different in two consecutive tests. The first test with 600 W power gave slower wetting than in the subsequent test with 1200/1800 W power despite the desiccation that is believed to have occurred in the hot test. The increased flow to Hole 3 is concluded to have been caused by a higher water pressure in the surrounding rock giving access to more water in the high-power test and quicker wetting of the buffer.

7.3 Tentative model for the wetting of the buffer

Case with hole-intersecting 4th order discontinuities

4th order fractures intersecting the holes bring in water quicker than the rock matrix. As soon as water flows in from a fracture it is adsorbed by the strongly hydrophilic buffer clay, which expands and seals off the fracture, partly by penetrating into openings with larger aperture than about 150 µm [10], and partly by blocking the apertures. The water pressure in the fracture is consequently raised here and water will flow more easily to the EDZ and to "activated" discontinuities of higher orders in the rock surrounding the holes. Hence, buffer clay that is in contact with these secondary structural features is supplied with water and they in turn tend to become blocked by expanding buffer clay. Many of the secondary discontinuities of 5th and 6th orders are estimated to have an average aperture that does not allow expanding clay to move into them (<150 µm) and they will therefore continue to serve as a water source throughout the maturation of the buffer clay and beyond this period.

As soon as the density of the clay in contact with water moving in from discrete discontinuities has risen to about 1700 kg/m^3, its hydraulic conductivity (E-12 m/s) is lower than that of the most shallow boring-disturbed rock zone and the lower flow resistance provided by this zone then causes redistribution of inflowing water over the entire periphery. This is valid for groundwater with a low electrolyte content, while the density of clay saturated with saline water may have to be about 1900 kg/m^3 for giving the same effect. One concludes from this that access to water in the saturation phase should be very uniform over the entire hole periphery. It is obvious that water available for saturation of the clay is entirely dependent on the flow capacity of the 4th order fractures and the water pressure in them.

Case with no hole-intersecting 4th order discontinuities

If no water-bearing 4th order fractures intersect the holes water for saturation of the buffer clay is provided only by the system of the continuous boring-disturbed zone including "activated" 5th and 6th order fractures. The wetting process may be different from that in the case with hydraulically active 4th order fractures in the sense that water may be absorbed by the clay matrix from the air with 100 % RH in the buffer voids. This process will cause slower wetting and expansion but is expected to be associated with the same initial blocking of wetter spots and redistribution of water as in the 4th order case.

The water available for saturation of the clay is entirely dependent on the flow capacity of the boring-disturbed zone with the integrated 5th and 6th order fractures and the water pressure in them. The wetting rate may be very much lower than in the case with water-bearing 4th order fractures.

8 REFERENCES

1. **Pusch R, Nilsson J, 1983.** Buffer Mass Test – Site documentation. Stripa Project Int. Rep. 83-04, SKB, Stockholm.

2. **Pusch R, Börgesson L, Ramqvist G, 1985.** Final Report of the Buffer Mass Test – Volume II: test results. Stripa Project Technical Report TR 85-12, SKB, Stockholm.

3. **Börgesson L, Pusch R, Fredriksson A, Hökmark H, Karnland O, Sandén T, 1991.** Final Report of the Rock Sealing Project – Sealing of the near-field rock around deposition holes by use of bentonite grouts. Stripa Project Technical Report TR 91-34, SKB, Stockholm.

4. **Pusch R, 1998.** Categorization of discontinuities for conceptual description of rock hosting repositories for hazardous waste. Eng. Geology, Vol.49 (pp.177-183).

5. **Chan T, Guvanasen V, Littlestone N, 1981.** Numerical modeling to assess possible influence of the mine openings on far-field in situ stress measurements at Stripa. Swed.-Amer. Coop. Program on Radioact. Waste Storage in Mined Caverns in Crystalline Rock. LBL-12469, SAC-33, UC-70.

6. **Pusch R, 1995.** Rock Mechanics on a Geological Base. Developments in Geotechnical Engineering, 77, Elsevier Publ. Co (ISBN:0-444-89613-9).

7. **Pusch R, 1998.** Practical visualization of rock structure. Engineering Geology, 49 (pp.231-236).

8. **Gale J, Witherspoon P A, Wilson C R, Roleau A, 1982.** The ”Macropermeability Experiment”. Geological Disposal of Radioactive Waste. In-situ exepriments in granite. Proc. Of the OECD/NEA Workshop, Stockholm October 25-27 1982.

9. **Olkiewicz A, Gale J E, Thorpe R, Paulsson B, 1979.** Geology and fracture system of Stripa. Swedish-American Cooperative Program on Radioactive Waste Storage in Mined Caverns in Crystalline Rock. LBL-8907, SAC-21, UC-70.

10. **Pusch R, Börgesson, L, Fredriksson A, Markström I, Erlström M, Ramqvist G, Gray M, Coons W, 1988.** Rock Sealing – Interim Report on the Rock Sealing Project (Stage I). Stripa Project Technical Report TR 88-11, SKB, Stockholm.

11. **Pusch R, 1997.** SKB Arbetsrapport: AR D-97-05 "Boring-induced Disturbance of Granitic Rock". SKB, Stockholm.

12. **Liedtke L, 2001.** Prel. Information form BGR field tests at AEspoe, September-October, 2001.

13. **Siitari-Kauppi M, Autio J, 1998.** Investigation of rock porosity and microfracturing with ^{14}C-PMMA method. SKB Djuptförvar, Project Report PR D-98-02.

14. **Pusch R, Neretnieks I, Sellin P, 1991.** Description of pathways in a KBS-3 type repository. SKB Technical Report TR 91-49, SKB, Stockholm.

APPENDIX

BMT data for modelling purposes

Rock

- Granitic
- Density 2700 kg/m^3
- Thermal conductivity 3.6 W/m,K, heat capacity 800 Ws/kg,K
- Hydraulic conductivity (Bulk E-11 to E-10 m/s)

Groundwater

Slightly brackish with Ca and Mg as dominating cations in certain areas where the total salt content was found to be about 120 ppm, and Na in others where the totalt salt content was about 310 ppm. pH was around 7.

Heater holes

Diameter 0.76 m, Length (vertical) 3.2 meters as an average.

Heaters

- Length 1.52 m (with shaft for power cable at the top, and piedestal for support)
- Diameter 0.38 m
- Power 600 to 1800 W in the tests
- Thermal conductivity 59 W/m,K, heat capacity 460 Ws/kg,K
- Density 7800 Kg/m^3

Buffer blocks of MX-80

Physical properties are the same as for the Prototype Repository. The dimensions and densities were:

Holes 1, 2 and 5 ("wet holes"):

- Outer diameter 0.74 m, inner diameter 0.19 m
- Density with 10 % water content, 2070-2110 kg/m^3

Holes 3,4 and 6 ("dry holes"):

- Outer diameter 0.70 m, inner diameter 0.19 m
- Density with 13 % water content, 2090-2140 kg/m^3

Geometry of holes

Holes 1, 2 and 5 ("wet holes"): Gap between blocks and rock wall = 1 cm, water-filled very soon. Gap between blocks and heaters almost none.

Holes 3,4 and 6 ("dry holes"): Gap between blocks and rock wall = 3 cm, filled with MX-80 powder with 10 % water content to a density of 1200 kg/m^3.

Backfill

- Density: The upper part of the heater holes contained on-site compacted backfill consisting of a mixture of silty/sand mixed with 10 % (by weight) of MX-80 bentonite with 10 % water content. The average density of this mixture after application was found to be 1820 to 2200 kg/m^3. For modelling purposes it can be taken as 2000 kg/m^3.
- The hydraulic conductivity can be taken as E-9 m/s
- The swelling pressure can be taken as 200 kPa
- The compressibility can be evaluated from laboratory tests that gave 2 % compression for an axial load of 500 kPa of unsatured material. At saturation the swelling pressure determines the compressibility.
- Thermal conductivity 1.5 W/m,K, heat capacity 1200 Ws/kg/K